EVOLUTIONARY BIOLOGY

Ecological interactions and genomic innovation fueled the evolution of ray-finned fish endothermy

Fernando Melendez-Vazquez[1], Alexander G. Lucaci[2,3]†, Avery Selberg[4]†, Julien Clavel[5], Melissa Rincon-Sandoval[6], Aintzane Santaquiteria[6,7], William T. White[8], Danielle Drabeck[9], Giorgio Carnevale[10], Emanuell Duarte-Ribeiro[11], Masaki Miya[12], Mark W. Westneat[13], Carole C. Baldwin[14], Lily C. Hughes[15,16], Guillermo Ortí[7], Sergei L. Kosakovsky Pond[4], Ricardo Betancur-R[1], Dahiana Arcila[1]*

Endothermy has independently evolved in several vertebrate lineages but remains rare among fishes. Using an integrated approach combining phylogenomic and ecomorphological data for 1051 ray-finned fishes, a time-dependent evolutionary model, and comparative genomic analyses of 205 marine vertebrates, we show that ecological interactions with modern cetaceans coincided with the evolution of endothermy in ray-finned fishes during the Eocene-Miocene. This result is supported by evidence of temporal and geographical overlap between cetaceans and endothermic fish lineages in the fossil record, as well as correlations between cetacean diversification and the origin of endothermy in fishes. Phylogenetic comparative analyses identified correlations between endothermy, large body sizes, and specialized swimming modes while challenging diet specialization and depth range expansion hypotheses. Comparative genomic analyses identified several genes under selection in endothermic lineages, including *carnmt1* (involved in fatty acid metabolism) and *dcaf6* (associated with development). Our findings advance the understanding of how ecological interactions and genomic factors shape key adaptations.

INTRODUCTION

Endothermy, the ability to generate heat via metabolic processes and maintain an elevated body temperature independent of environmental conditions, is one of the most notable adaptations in vertebrates (*1*, *2*). This trait has independently originated in birds and mammals, as well as in some reptile and fish lineages (*3*). Although endothermy is considered a functional innovation in fishes, this capability is present in less than 0.1% of the roughly 36,000 known fish species (*4*). Ray-finned fishes have independently evolved endothermy at least four times (*1*, *3*). These include the generation of internal heat in the eye and brain region (butterfly kingfish, sailfishes, marlins, and swordfishes), red muscle (some tunas), a combination of regional strategies (Pacific bluefin tuna, slender tuna, among others), or full-body endothermy (opahs) (*3*, *4*). Certain endothermic fishes can conserve the heat they generate internally using the retia mirabilia (*5*). This structure uses a countercurrent mechanism for heat retention, reducing heat dissipation (*5*).

The diverse manifestations and mechanisms of endothermy in fishes present substantial challenges to their study, particularly compared to terrestrial vertebrates (*6*). Previous hypotheses on the evolutionary advantages of endothermy in fishes included enhanced aerobic swimming performance (*7*, *8*), thermal and depth range expansion (*5*, *9*–*11*), specialized diets (*5*, *12*), increased body size (*13*, *14*), and higher metabolic rates (*4*, *15*), often in conjunction with ancient paleoclimatic events such as ocean cooling during the Cenozoic (*4*, *16*). Past studies, which often suffered from limited taxonomic sampling (*7*, *17*), analyzed one or more of these hypotheses, typically using a small number of endothermic fish lineages (*5*). Furthermore, the lack of statistical methods capable of incorporating time-dependent evolutionary processes has hindered experiments from rigorously quantifying how ancient climatic changes and other time-varying factors influenced the evolution of endothermy in fishes. Although discussions on the evolution of endothermy in ray-finned fishes in relation to the geological past have largely focused on paleoclimatic changes (*4*), a broader analysis of its evolutionary and geological context has revealed an often-overlooked phenomenon. Ecological interactions (i.e., competition, predation, etc.) (*18*) have been linked to increased body sizes and the potential evolution of endothermy in organisms like elasmobranchs (*14*), synapsids (*19*), and archosaurs (*19*). Yet, the view on interactions related to endothermy in ray-finned fishes often centers on endothermic organisms outcompeting ectothermic ones (*7*, *17*). However, these hypotheses ignore the fact that despite being formidable apex predators (*1*, *4*), endothermic ray-finned fishes are not considered the most competitively dominant endothermic organisms in the ocean. Consequently, the potential for evolutionary arms races through ecological interactions among marine vertebrates during the Eocene-Miocene remains underexplored. The Eocene-Miocene transition was a period of substantial marine ecosystem restructuring marked by the expansion of

[1]Scripps Institution of Oceanography, University of California, San Diego, 9500 Gilman Drive, La Jolla, CA 92093-0244, USA. [2]Department of Physiology and Biophysics, Weill Cornell Medicine, New York, NY 10021, USA. [3]The HRH Prince Alwaleed Bin Talal Bin Abdulaziz Alsaud Institute for Computational Biomedicine, Weill Cornell Medicine, New York, NY 10021, USA. [4]Institute for Genomics and Evolutionary Medicine, Temple University, Philadelphia, PA 19122, USA. [5]Université Claude Bernard Lyon 1, LEHNA UMR 5023, CNRS, ENTPE, F-69622 Villeurbanne, France. [6]University of Oklahoma, 730 Van Vleet Oval, Richards Hall, Norman, OK 73019, USA. [7]Department of Biological Sciences, The George Washington University, Washington, DC 20052, USA. [8]Commonwealth Scientific and Industrial Research Organisation (CSIRO) Australian National Fish Collection, National Research Collections Australia, Hobart, TAS 7001, Australia. [9]University of Minnesota Twin Cities, 1475 Gortner Ave., St. Paul, MN 55108, USA. [10]Dipartimento di Scienze della Terra, Università degli Studi di Torino, 10124 Torino, Italy. [11]University of Basel Zoological Institute, Vesalgasse 1, Basel CH 4051, Switzerland. [12]Natural History Museum and Institute, Chiba, Chiba 260-8682, Japan. [13]Department of Organismal Biology and Anatomy, The University of Chicago, Chicago, IL 60637, USA. [14]National Museum of Natural History, Smithsonian Institution, Washington, DC 20560, USA. [15]Department of Marine, Earth, and Atmospheric Sciences, North Carolina State University, 2800 Faucette Boulevard, Raleigh, NC 27607, USA. [16]North Carolina Museum of Natural Sciences, 11 W Jones Street, Raleigh, NC 27601, USA.
*Corresponding author. Email: dkarcila@ucsd.edu
†These author contributed equally to this work.

open-ocean predatory niches, the diversification of cetaceans, and shifts in oceanic productivity (*20*, *21*). The appearance of marine cetaceans created additional ecological niches and resource pressures for existing apex ray-finned fish predators (tunas, billfishes, and opahs), suggesting that factors like coevolution or competitive exclusion might have shaped their ecological roles. Given the potential for competition-driven endothermy and the dietary and geographic overlap between cetaceans and endothermic ray-finned fishes (*22*–*24*), this underexplored aspect of marine vertebrate interaction merits further investigation.

Affordable genome sequencing technologies greatly advanced the study of fish endothermy. A whole-genome comparison of billfishes and tunas identified signatures of positive selection in genes related to metabolic and cell pathway regulation (*25*). Notably, *atp2a1* and *atp2a1l* have emerged as key genes involved in pumping calcium ions (Ca^{2+}) into the sarcoplasmic reticulum, a critical process in muscle contraction and internal heat production (*1*, *25*). A study in tunas observed mutations in the *gpd1b* and *gpd1c* genes, contributing to ATP synthesis and a high rate of oxidative phosphorylation, generating localized heat in the tissue (*26*). In opahs, the only fishes with whole-body endothermy, a previous experiment identified positive selection signals in *ndufa10* and *cox15* genes, which play a role in the mitochondrial electron transport chain, a process integral to oxygen reduction, creating high-energy phosphate bonds from ATP, resulting in heat generation (*27*). Despite the progress that previous genomic studies have achieved, the limited inclusion of endothermic species, coupled with a lack of phylogenetic replication across multiple endothermic lineages, remains a substantial limitation (*25*–*28*). By incorporating more endothermic fishes and marine vertebrates, comprehensive genomic analyses might reveal the convergent molecular underpinnings of marine endothermic lineages. However, identifying orthologous sequences at deep evolutionary scales remains a major challenge (*29*).

Using a multifaceted approach, we investigate the evolutionary origins of endothermy within ray-finned fishes. First, we constructed the largest time-calibrated phylogenomic tree for ray-finned fishes to date, encompassing 1051 species and including all known endothermic groups. Next, we built a comprehensive comparative dataset incorporating multiple ecomorphological indexes, including swimming mode (e.g., sub-carangiform, carangiform, and thunniform), an array of body shape metrics, diet preferences, and depth range to test for evolutionary correlations with endothermy. To explore the origins of ray-finned fish endothermy, we further developed and applied a time-variable model to independently evaluate two key factors: (i) its relationship with paleoclimatic changes and (ii) its association with the lineage diversity of fossil and extant cetaceans and chondrichthyans, as an avenue to assess the potential role of ecological interactions with marine vertebrates. In addition, we examined fossil assemblages from the past 40 million years (Myr) to investigate spatiotemporal overlaps among ancient pelagic communities. Last, we performed comparative genomic analyses using 205 long-read and short-read genomes encompassing all endothermic fish lineages and other marine vertebrates, including whales, penguins, and marine turtles, followed by positive selection and accelerated evolution analyses to detect genomic signatures of convergence.

RESULTS

Constructing a comprehensive phylogeny of ray-finned fishes

We addressed the limitations of previous studies, which focused on the origin of endothermy in small fish subclades (*5*, *7*, *17*), by using genome-wide data to generate a phylogenomic hypothesis for a large group of ray-finned fishes (Fig. 1). Our genomic dataset includes 1099 single-copy nuclear exon markers (*30*) (dataset S1) sequenced from 1051 species, spanning all four major endothermic lineages represented by 22 species (table S1). Our resulting phylogeny was time calibrated using a congruification approach (*31*), which integrates multiple secondary calibrations from existing time trees based on shared taxa (see Materials and Methods). We used the time tree from Hughes *et al.* (*30*) as the primary framework but supplemented it with eight additional calibrations from four calibration schemes derived from more recent studies (*30*, *32*–*40*) to refine divergence time estimates for major fish clades (Fig. 1, fig. S1, and table S2). To address uncertainties in phylogenetic placement and divergence times, we generated alternative topologies and calibration strategies using four randomly grouped genomic subsets (*41*), each comprising ~220 loci, resulting in a total of 19 time-calibrated trees used for downstream comparative analyses (datasets S2 to S6). This set of ray-finned fish phylogenies is the most phylogenomically exhaustive to date, with a comprehensive representation of all endothermic lineages.

Evolutionary dynamics of endothermy

To elucidate the origins and effects on lineage diversification of endothermy in ray-finned fishes, we used a stochastic character mapping of discrete traits (SIMMAP) (*42*) and state-dependent diversification and extinction analyses based on hidden states (HiSSE) (*43*). Aligning with previous assessments of the origin of endothermy in ray-finned fishes (*25*–*27*, *32*), our SIMMAP results corroborate four independent origins of endothermy within three distantly related clades: one in the stem lineage leading to Istiophoriformes (sailfishes, marlins, and swordfishes), another in Lampriformes, and two independent origins within the family Scombridae (one in the tunas and one in the butterfly kingfish *Gasterochisma melampus*) (Fig. 1). HiSSE analysis (dataset S7) favors a character-independent model with four hidden states [CID-4; Akaike information criterion weight (AICw) > 99%]. This result suggests that, although hypothesized as a key innovation (*44*) contributing to both the avian and mammal's evolutionary success (*14*, *19*), endothermy is not a major factor influencing ray-finned fishes' diversification dynamics. Endothermy's scattered phylogenetic presence, distinct evolutionary patterns, and lack of association with increased rates of evolution reflect features often associated with evolutionary dead ends. Although our methods were not able to account for elevated extinction rates for endothermic species (Fig. 1 and dataset S7), they do appear to correlate with the phylogenetic patterns observed from potential loss/gain imbalances (*45*). This phenomenon is similar to the evolution of red flowers (*45*), where, despite multiple origins, the trait is not widespread due to a higher loss rate. This suggests that, although endothermy may provide a short-term evolutionary advantage, it is not more common due to high maintenance costs outweighing the potential benefits under most conditions.

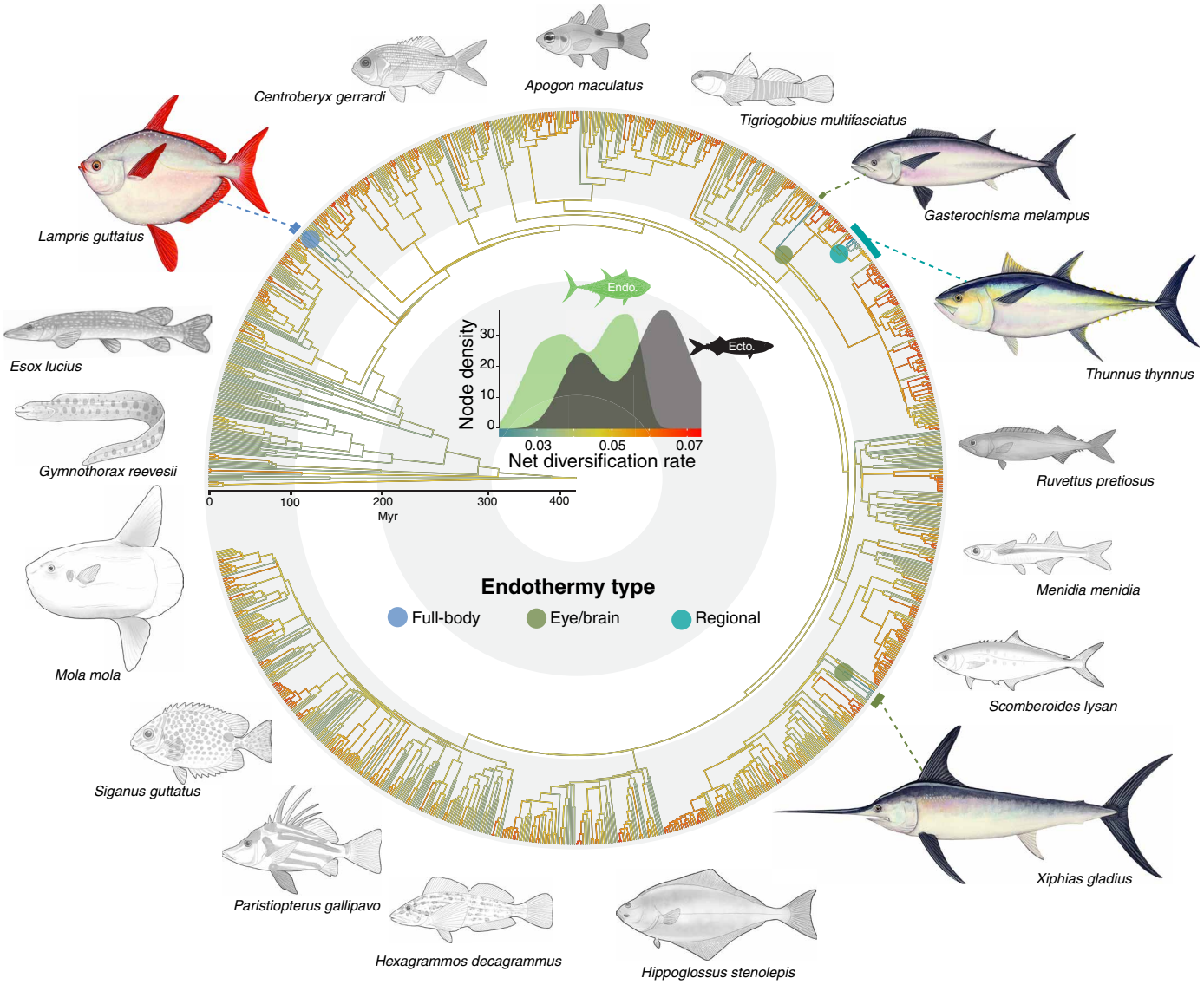

Fig. 1. Time tree of 1051 species of ray-finned fishes. Tree based on 1099 single-copy nuclear exon markers. Colored fish illustrations indicate endothermic lineages, whereas grayscale illustrations represent their ectothermic counterparts. Colored dashed lines indicate endothermic lineages and the type of endothermy they exhibit. Colored branches show net diversification rates for all 1051 species, estimated using HiSSE. The central graph compares the distribution of diversification rates between endothermic and ectothermic ray-finned fishes. Illustration(s) by Julie Johnson (Life Science Studios).

Ecomorphological predictors of endothermy evolution

We assembled a combined dataset encompassing four key ecomorphological traits from multiple databases (see Materials and Methods), including swimming mode, diet preference, depth range, and body size (average standard length and length-weight relationship) (table S3). Historically, these traits have been linked to the evolution of endothermy in fishes (*1*, *4*, *5*, *12*, *17*). In addition, we used the FishShapes (FS) dataset (*46*), to examine lesser-studied relationships, including morphometric traits such as body depth, width, head depth, caudal peduncle width, and weight (table S4). To ensure robustness, we also retested average standard length using FS data. Because of the inconsistent classification of Istiophoriformes' swimming mode, we ran the swimming mode comparisons using two different schemes: classifying them as either sub-carangiform or thunniform swimmers (tables S5 to S8). From a kinematic perspective, traditional swimming mode categories (e.g., anguilliform, carangiform, thunniform, among others) are better represented as continuous traits based on undulatory movements (*47*). However, given the broad taxonomic scope of our study (>1000 species), we used these traditional categories as practical and applicable ecological descriptors. This approach remains common across comparative studies and is represented in several major databases (see Materials and Methods). We emphasize that these classifications are intended as broad, scalable proxies for locomotion, not precise biomechanical definitions of swimming behavior. To explore potential evolutionary correlations between endothermy and these traits, we conducted

phylogenetic generalized logistic regression (PGLR) analyses (*48*), both in univariate (uv) and multiple logistic regression (mr) frameworks. Because of analytical convergence issues, the multiple logistic regression tests focused on the four endothermy-linked traits but excluded the additional FS morphometric factors. Variations in tree topology and divergence times had negligible effects on comparative analyses (Fig. 2A). Last, to account for potential instances of false discovery, we implemented a false discovery rate (FDR) correction to all estimated *P* values.

Our analyses revealed a significant correlation between body size (average standard length) and the origin of endothermy (P_{uv} = 0.01 to 0.02; P_{mr} = <0.01 to 0.04) in ray-finned fishes. However, no significant correlation was found for the length/weight relationship, suggesting different selective pressures on these traits. In addition, we detected no significant correlation between endothermy and depth range (P_{uv} = 0.24 to 0.99; P_{mr} = 0.06 to 0.17) or specialized diets (P_{uv} = 0.25 to 0.80; P_{mr} = 0.12 to 0.99). These findings appear to differ from the established hypotheses concerning the evolution of endothermy and extrinsic ecological factors (*1*, *5*, *17*, *49*), revealing that the evolution of endothermy was not influenced by the need for enhanced access to different depths (*1*, *4*, *9*, *10*) or dietary changes (*5*, *12*).

No significant correlation was observed for swimming mode in univariate tests (P_{uv} = 0.68 to 0.99), but a significant relationship emerged in multiple logistic regression tests (P_{mr} = 0.02 to 0.04). This result identified swimming mode as a significant predictor of endothermy in interactions with other traits (Fig. 2A). Analyses using the FS dataset (Fig. 2A) showed significant correlations between endothermy and a broader caudal peduncle, deeper heads, taller and wider bodies, and greater body lengths (P_{uv} = <0.01 to 0.05). No significant correlations were found for mouth width, weight, body depth-length ratio, or body depth-length-weight ratio (table S5). Together, these results support an evolutionary association between endothermy in ray-finned fishes and size-related metrics like increased body length, depth, and width, along with distinct swimming modes (Fig. 2A and tables S5 to S8). Although these traits are common to large pelagic fishes and are not exclusive to endothermic species, the significant correlation between these traits and endothermy suggests that they may have been further influenced or more intensely selected in endothermic fishes. This could be due to the enhanced metabolic and physiological demands associated with endothermy, driving a stronger selection pressure for these traits in endothermic species compared to their ectothermic counterparts (*4*).

The relationship between past climatic changes and endothermy

Short-term and long-term temperature fluctuations have been hypothesized to influence endothermic adaptations in terrestrial (*6*) and marine (*4*, *5*) ecosystems. The evolution of endothermy in fishes has been associated with cooling periods during the Cenozoic (*4*). In addition, previous studies used proxies like paleo-altitude and paleo-latitude (*6*), movement tracking data (*17*), and dietary patterns (*5*) to identify similar climatic relationships. To directly assess the correlation between the evolution of endothermy and ancient climatic changes, we developed a phylogenetic comparative approach based on a modified threshold model. This model tests for a statistical association between the emergence of a discrete trait (i.e., endothermy) and a time-varying function (*50*) (i.e., temperature; see Materials and Methods). The model was validated through extensive simulations (figs. S2 to S11 and dataset S8), demonstrating high accuracy in detecting evolutionary signals. Although our time-dependent model receives some support (average Akaike weights AICw = 0.18), both random walk (Brownian motion, average AICw = 0.32) and phylogenetic signal (Lambda, average AICw = 0.27) models are favored (Table 1 and tables S9 and S10). This suggests that evidence for the role of climate in the evolution of endothermy is equivocal at best.

Cetacean interactions as a selective pressure in the origin of fish endothermy

The concept of ecological interactions and evolutionary arms races driving the origin of endothermy is not unexpected; it has been suggested in synapsids and archosaurs during the Triassic (*19*). Similarly, ecological interactions with giant, planktivorous bony fishes have been used to explain thermoregulatory strategies and patterns of gigantism in some elasmobranchs (*14*). The Cenozoic, particularly the Eocene-Miocene period, exhibits similar trends indicative of big changes in the pelagic realm. This period was marked by mammal recolonization of the ocean (*51*), the presence of endothermic chondrichthyan lineages, and the origin of endothermy in pelagic ray-finned fishes (Fig. 2A). These larger endothermic organisms had heightened metabolic requirements, overlapping diets (i.e., small fishes, plankton, squids, and some crustaceans) (*22*, *23*), and a need for increased quantities of food, likely influencing their evolutionary trajectories (*22*–*24*). However, the hypothesis that whales and ray-finned fishes had ecological interactions similar to those between synapsids and archosaurs has not been explored. Establishing direct evidence for ecological competition between high-performance endothermic fishes and cetaceans is inherently challenging. However, contemporary fishery studies have identified a substantial niche overlap between endothermic fishes and cetaceans (*24*, *52*). Furthermore, satellite tracking data provide evidence that some endothermic fishes and marine mammals exhibit remarkably similar migration ranges (*17*), suggesting that both can access the same productive feeding grounds, they can maintain activity in both warm and cold waters, and they share physiological capabilities that allow them to track and exploit the same mobile prey resources (*22*, *23*) across ocean basins, providing strong evidence for niche overlap and ecological interactions.

To investigate the relationship between the evolution of endothermy in ray-finned fishes and the evolutionary trends of modern cetaceans, we conducted model-fitting analyses using our proposed time-varying threshold model. Instead of using paleoclimatic curves as input, we fitted the model with lineage through time (LTT) curves, which depict the accumulation of lineages over time, and diversification through time (DTT) curves, which track species richness and incorporate speciation and extinction, based on fossil and extant species data for modern cetaceans (Neoceti) (*51*) and chondrichthyans (*53*, *54*). This approach enabled us to directly assess whether evolutionary dynamics in these external groups correlate with the emergence of endothermy in ray-finned fishes. Because of the time-varying nature of the model, we empirically validated it by fitting two additional trees with artificially younger evolutionary origins for endothermy. These branch length alterations assigned more recent temporal origins (25 and 50%) for endothermic ray-finned fish lineages. The goal was to assess the robustness of our analyses: If positive results were obtained using trees younger than the estimated origin of endothermy, it would indicate that the model had not adequately captured the effect. Conversely, if the model

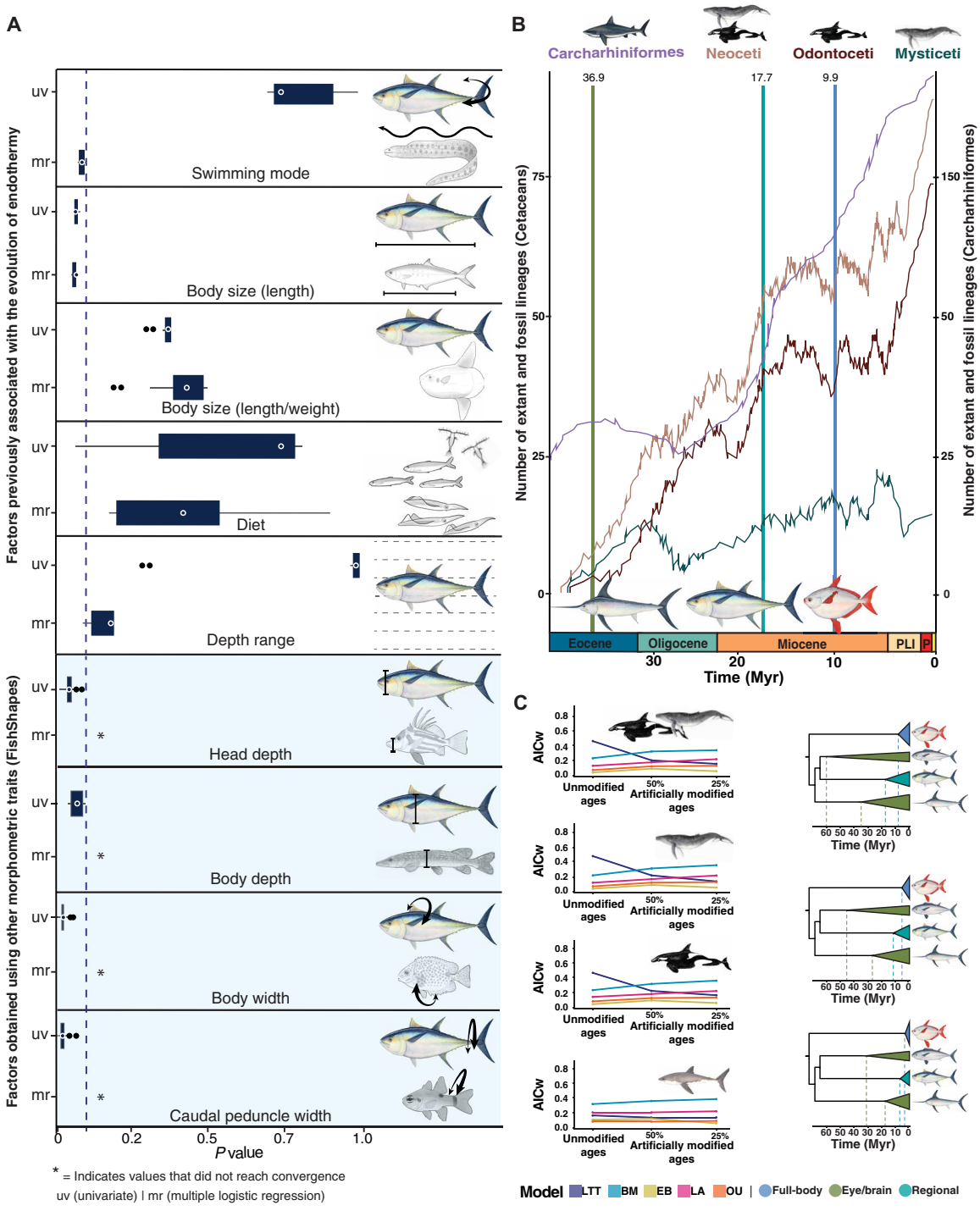

Fig. 2. Evolutionary correlations and tests for ecological interactions. (**A**) Results illustrating nine sets of boxplots, each representing either one of the factors previously associated with the evolution of endothermy (white shaded) or one of the statistically significant factors obtained using additional morphometric traits (FS dataset) (blue shaded). The vertical dashed line represents the threshold for statistical significance (*P* value of 0.05). The vertical axis indicates whether the analysis was performed on a single trait (uv) or considering all traits jointly (mr). Each boxplot encompasses the distribution of the results of the PGLR analyses for the 19 different trees estimated to account for phylogenetic uncertainty. (**B**) LTT plots for all cetacean groups combined (Neoceti), Odontoceti, Mysticeti, and Carcharhiniformes, based on previously published phylogenies that include fossil and extant species. The vertical lines intersecting the LTT plots denote the origin of endothermic fish lineages. (**C**) AICw comparisons between our calibrated phylogeny (unmodified) and our artificially modified ages for the origin of endothermy (25 and 50% younger) for all four major ray-finned fish groups. Artificially modified ages accounted for any positive correlation biases introduced by our model or curves. Phylogenies on the right side of the panel illustrate the temporal differences in the origin of endothermy among the trees used. BM, Brownian motion; EB, Early Burst; LA, Pagel's Lambda; OU, Ornstein-Uhlenbeck. Illustration(s) by Julie Johnson (Life Science Studios).

detected a signal using only our tree but not with artificially younger trees, it provides more confidence in the results. We also attempted to run the model with artificially older origins for endothermy, but the runs failed to converge because most transitions were pushed beyond the appearance of cetacean lineages. The cetacean LTTs were analyzed in three ways: Mysticeti only (baleen whales), Odontoceti only (toothed whales), and Neoceti (baleen and toothed whales). This approach was taken to further discern the origin of the effect being observed and to avoid potential instances of false positives. The chondrichthyans LTTs and DTTs were based on either Carcharhiniformes (*54*) only or all chondrichthyans (*53*). We excluded Odontoceti and Mysticeti from the DTT analysis because DTT estimation requires ultrametric trees, and removing fossil tips lowers taxonomic sampling (<100 species), which could have compromised the model's accuracy, as indicated by our simulations (figs. S2 to S11).

Model fitting results indicate an evolutionary correlation between the origin of endothermy in ray-finned fishes, LTT and DTT trends of Neoceti, and LTT trends in Odontoceti and Mysticeti (AICw ~ 0.43), suggesting that the diversification of modern whales in the marine environment greatly restructured the ecological and biological dynamics of the ocean, particularly among large pelagic marine organisms (Table 2). Visual inspection of the LTT curves for Neoceti, Odontoceti, and Mysticeti (Fig. 2B) reveals multiple inflection points, marked by bursts, plateaus or slowdowns, and subsequent bursts, that closely align with the origins of endothermy in ray-finned fishes. The first inflection, during the late Eocene to early Oligocene (~38 to 30 Myr), features a slowdown followed by a burst across all cetacean groups analyzed, coinciding with the emergence of Istiophoriformes. A second inflection during the early to mid-Miocene (~23 to 16 Myr) aligns with the appearance of Scombriformes, and a third inflection in the late Miocene (~11 to 7 Myr) corresponds with the origin of Lampriformes. Although Carcharhiniformes also exhibit increasing lineage accumulation, they lack the punctuated burst-slowdown-burst patterns observed in cetaceans (Table 2). Notably, Mysticeti shows the best model fit despite a shallower slope, possibly because its mid-Miocene inflection aligns with endothermic transitions. These results suggest that the timing and structure of diversification bursts in cetaceans, rather than absolute richness, correlate with the emergence of endothermy in ray-finned fishes.

As major marine predators, cetaceans may have introduced additional ecological pressures for resources, which potentially played a crucial role in the evolution of endothermy in ray-finned fishes. This finding aligns with the demonstrated performance advantages in endothermic fishes, particularly their higher cruising speeds (*7*, *8*, *17*) and sustained cardiovascular capabilities (*55*), supporting our hypothesis on the role of competitive interactions in pelagic environments. Although these results suggest that ecological interactions played a role in the origin of endothermy, they also underscore the complexity of this trait and the numerous factors that contributed to its development (Supplementary Text). Although our LTT- and DTT-based models present a moderate AICw (~0.43) value for Neoceti, these results are consistent with our simulations when the strength of the signal/effect was low (fig. S2 and tables S9 and S10) (*56*), leading to conservative AICw estimates even when we induced the desired correlation effect. This relatively low signal/effect strength can also be explained by the small number of transitions to endothermy in ray-finned fishes ($n = 4$). Furthermore, when we tested our model by artificially altering the ages of endothermic ray-finned fish lineages, our analyses found no correlation.

Table 1. Results of model fitting for climatic analyses. Average weighted Akaike scores (AICw) for different models, including our time-dependent (Clim), Brownian motion (BM), Early Burst (EB), Pagel's Lambda (Lambda), and Ornstein-Uhlenbeck (OU) models, along with averages for beta (β), and lambda (λ) values. Bold values indicate the best-supported model for each climatic curve based on AIC weights.

Curve	Clim AICw	BM AICw	EB AICw	Lambda AICw	OU AICw	β	λ
Scotese Deep	0.201	**0.312**	0.113	0.263	0.111	−2.295	0.959
Scotese GAT	0.201	**0.312**	0.113	0.263	0.111	−2.298	0.959
Scotese Polar	0.199	**0.313**	0.113	0.263	0.112	−2.002	0.959
Scotese Tropical	0.127	**0.339**	0.123	0.290	0.121	−1.364	0.959
Total average	0.182	**0.319**	0.115	0.270	0.114	−1.990	0.959

Table 2. Results of model fitting for ecological interactions. Average weighted Akaike values (AICw) for each model based on LTT curves for cetaceans (whole group, Mysticeti, and Odontoceti), Chondrichthyes, and Carcharhiniformes, along with averages for beta (β), mu (μ), and lambda (λ) values. Bold values indicate the best-supported model for each group based on AIC weights.

Group	LTT AICw	BM AICw	EB AICw	Lambda AICw	OU AICw	β	μ	λ
Mysticeti	**0.445**	0.227	0.083	0.145	0.099	0.344	−16.038	0.938
Odontoceti	**0.420**	0.237	0.087	0.152	0.104	0.237	−16.307	0.938
Cetaceans	**0.414**	0.239	0.088	0.153	0.105	0.216	−16.047	0.938
All Chondrichthyes	0.177	**0.336**	0.124	0.215	0.147	−0.143	−9.497	0.938
Only Carcharhiniformes	0.239	**0.311**	0.114	0.199	0.136	0.118	−20.694	0.938

Our time-dependent model was less favored (AICw ~ 0.28) and was outperformed by Brownian motion (AICw ~ 0.45) (Fig. 2, B and C, and tables S11 to S16). We observed no correlation between endothermic ray-finned fishes and the chondrichthyan and Carcharhiniformes LTT and DTT curves (Fig. 2, B and C; Table 2; and tables S11 to S16), providing additional evidence that the Eocene-Miocene, and not the Cretaceous, was a notable period for the evolution of endothermic strategies in ray-finned fishes. The lack of correlation observed in our analyses of chondrichthyan, Carcharhiniformes, and on our altered dates reinforces that the correlation observed with cetaceans obtained with the unmodified ages are unlikely to be false positives introduced by our model or the curves used. In addition, the timing of endothermy evolution in ray-finned fishes coincides with the radiation of cetaceans, with both groups representing small but notable portions of their respective vertebrate classes. Although earlier marine predator extinctions (plesiosaurs and mosasaurs, ~66 Myr) predate the evolution of endothermy in most ray-finned fishes, others like the Megalodon (3.6 Myr) show no correlation with our DTT and LTT curves (Fig. 2C and Table 2).

To further investigate the macroevolutionary history of ecological interactions between modern cetaceans and ray-finned fish endothermic lineages, we analyzed fossil records from the past 40 Myr using their historical biogeographic occupancy overlap. A failure to see an overlap between them would mean there were no interactions between the groups (*57*), making it unlikely that modern cetaceans promoted the origin of endothermy in ray-finned fishes. We examined a total of 12 geological formations, including fossil lineages for three main groups: Neoceti, endothermic chondrichthyans (Alopiidae and Lamnidae), and ray-finned fishes (Scombriformes, Istiophoriformes, and Lampridae). In addition, we included fossil data for two ray-finned fish lineages, Clupeiformes and Myctophiformes, which are well represented in geological formations and are prey for these marine predators (Fig. 3). These prey fossils were added to establish a historical dietary correlation to supplement the geographical correlation observed and further strengthen the feasibility of such ecological interactions taking place. Although most geological formations presented a temporal and geographic overlap of at least four of our six fossil lineages, two formations (the Yorktown and Monterey) included all six of them. These results further confirm the ancient coexistence of these marine apex predators. Although no macroevolutionary studies have explicitly considered the early trophic interactions between cetaceans and ray-finned fishes, our study provides evidence that the

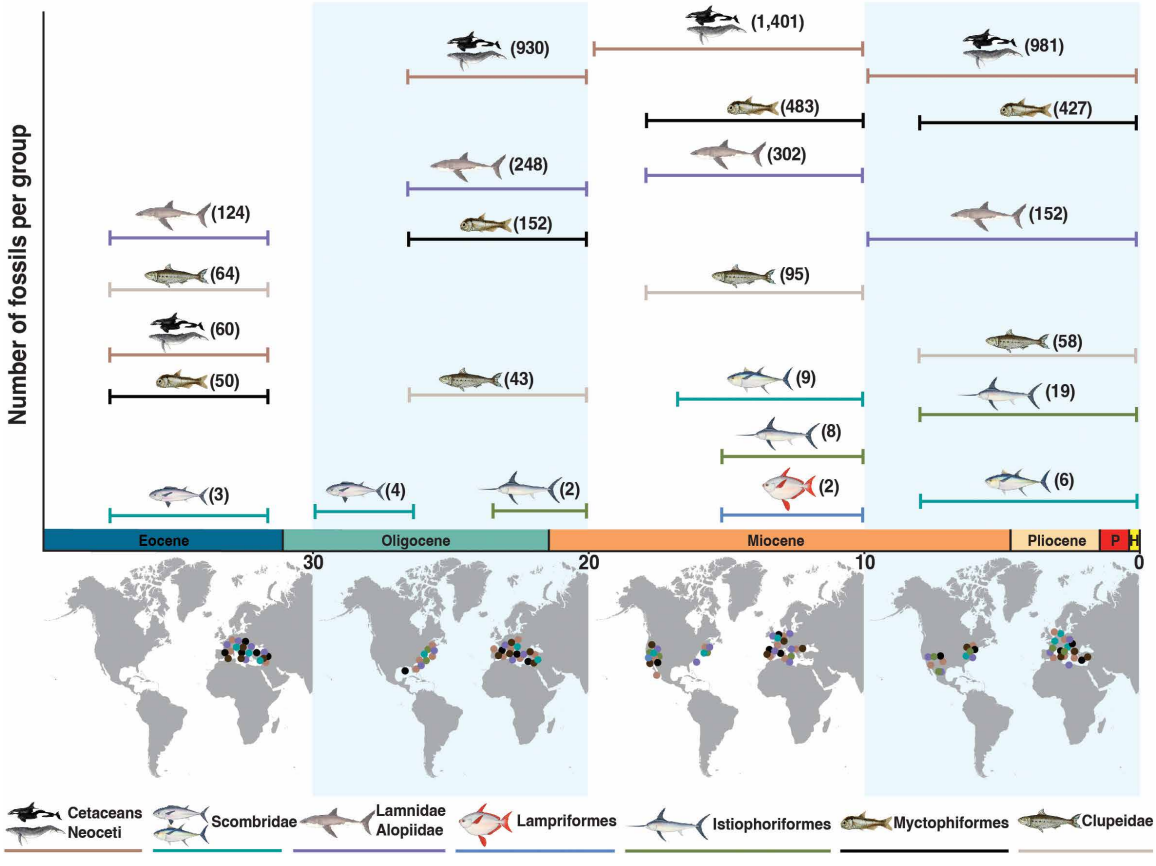

Fig. 3. Fossil evidence of geographic coexistence between cetaceans and fishes. Fossil record representations showing the geographical coexistence among different groups of predators and prey, suggesting potential ecological interactions among them. Major predators, alongside their correlated prey, were selected. Fossilized prey was included to support the observed geographical link to dietary ones, reinforcing the likelihood of such ecological interactions taking place. Each map represents intervals of 10 up to ~40 Myr, with dots indicating fossil location. Only regions with the simultaneous presence of at least four of our six fossil lineages are illustrated to maintain figure clarity. The intervals above the map indicate the fossil range age, and the number next to the silhouettes shows the fossils for each group and time range. Illustration(s) by Julie Johnson (Life Science Studios).

Eocene-Miocene appears to be a hotspot for these ecological interactions between these two groups. This period represents stages of an evolutionary arms race that could have led to the evolution of endothermy in ray-finned fishes and their distinct adaptations, a phenomenon that mirrors the evolutionary arms race between synapsids and archosaurs, where both groups adopted different movement strategies and physiological adaptations (endothermy) as a competitive advantage in the aftermath of the Permian-Triassic mass extinction (*19*). We propose that endothermy in ray-finned fishes could have evolved as a response to the increased energetic demands stemming from emerging ecological interactions with cetaceans in the marine realm, representing a key physiological adaptation in lineages exhibiting ecomorphological traits typical of pelagic fishes (*24*). Our data suggest that cetacean interactions influenced endothermy in ray-finned fishes (Fig. 2B), but the butterfly kingfish highlights the trait's broader evolutionary complexity. Although its divergence may overlap with early cetacean diversification (*52*), variable divergence estimates (table S2) reduce confidence in its origin within our time-varying model. Moreover, some estimates align its origin with the extinction of large marine reptiles such as plesiosaurs and mosasaurs (~66 Myr), suggesting that these apex predators may have imposed ecological pressures similar to those from modern cetaceans. Furthermore, the rarity of endothermy and its uneven distribution among ray-finned fishes, primarily concentrated in tunas, pose additional challenges to fully resolving its evolutionary trajectory.

Comparative genomics reveals convergent molecular adaptations for endothermy

We conducted a comprehensive genomic analysis of 205 genomes from diverse endothermic marine lineages, including mammals, birds, reptiles, chondrichthyans, and ray-finned fishes. Integrating 138 long-read and 69 short-read genomes, we identified 833 single-copy orthologs along with 61 candidate genes associated with endothermic traits (*1*, *4*, *25*–*27*) in a dataset of 894 single-copy orthologous sequences (datasets S9 to S11). To detect positive selection, we used the BUSTED-E and BUSTED-PH models, modified versions of the BUSTED[S] model implemented in the HyPhy package (fig. S12) (*58*), which account for synonymous site-to-site substitution rate variation (SRV) (*59*, *60*). Following FDR corrections, genes were categorized based on their selection profiles: FDR-class 101 for genes selected in the foreground (fg) without background (bg) selection and FDR-class 111 for genes under positive selection in both the fg and bg, indicating varied selection pressures (Supplementary Text). Our analyses spanned four scenarios (S1 to S4), ranging from a broad comparison of all endotherms versus ectotherms (S1) to more specific contrasts between different groups of endotherms and ectotherms (S2 to S4). We observed 51 positively selected genes (PSGs) in scenario S1 (Fig. 4A), primarily affecting neural development, muscle function, and metabolism (*61*). In regional endotherms such as tunas and great white sharks (S2), we detected 17 PSGs (Fig. 4B), including those related to energy generation and muscle function (*61*). Scenario S3 highlighted seven

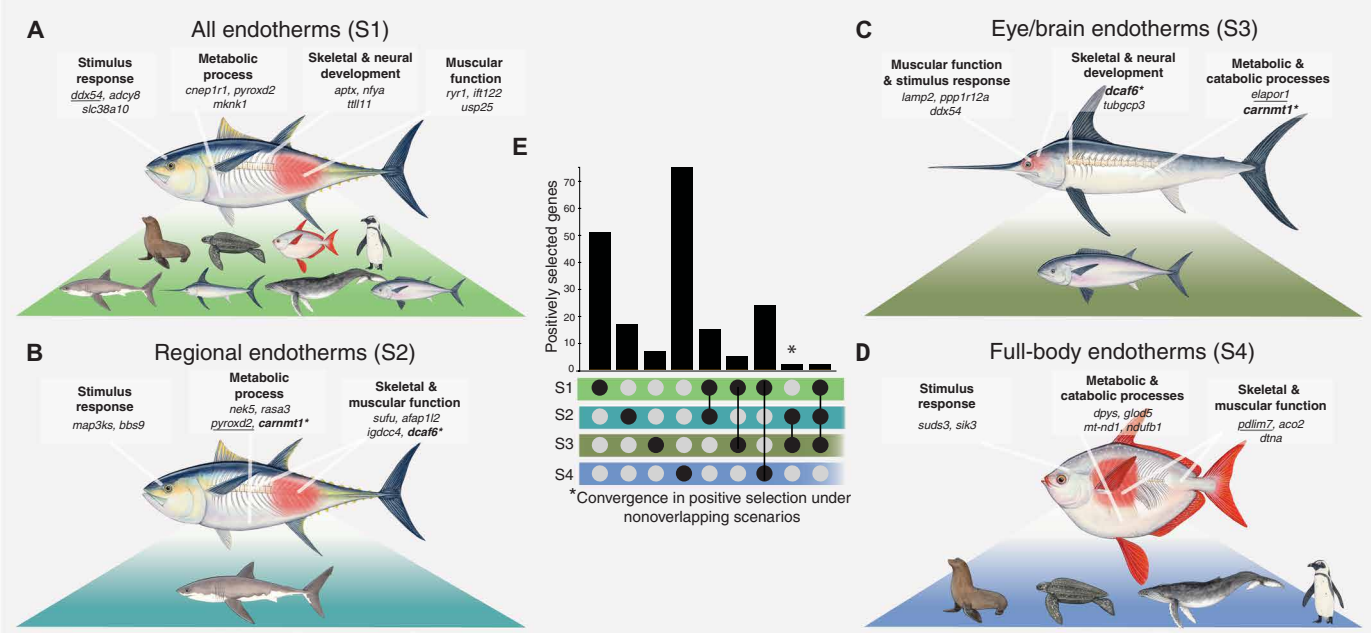

Fig. 4. Positive selection of endothermic genes. Genes that exhibited positive selection and accelerated relative rates of evolution across different scenarios using BUSTED-PH (corrected with BUSTED-E) and "RER." The genes with the highest evolutionary rate for each scenario are underlined. Genes showing convergent signals are marked with an asterisk (*). Each scenario highlights the vertebrates used as the foreground species. We also highlighted regions used for internal heat production associated with genes under selection. The scenarios are (**A**) all endothermic species (foreground or fg) compared to all ectothermic species (background or bg), (**B**) regional endotherms (fg), all ectotherms (bg), and the other endothermic representatives as nuisance species, (**C**) eye/brain endotherms (fg), all ectotherms (bg), and the other endothermic representatives as our nuisance species, and (**D**) full-body endotherms (fg), all ectotherms (bg), and the other endothermic representatives as our nuisance species. (**E**) Upset plot indicating the number of genes under positive selection for each scenario. Boxes with black dots joined by a black line represent the number of genes shared between those highlighted scenarios. Although shared genes were observed among all endothermic species, some genes showing signatures of selection and accelerated evolution were found exclusively in some scenarios. Functional categories based on Biological Processes were obtained using the PANTHER database. Illustration(s) by Julie Johnson (Life Science Studios).

PSGs in eye/brain endotherms, like billfishes and marlins (Fig. 4C), associated with catabolic processes and muscular maintenance (*61*). In full-body endotherms, including marine mammals and penguins (S4) (Fig. 4D), 75 PSGs were found to be related to metabolism and muscle contraction (tables S18 to S26) (*61*).

We expanded our positive selection analyses by estimating relative evolutionary rates (RERs) (*62*) through Hyphy (*58*) (fig. S17 and tables S18 to S26). This method uses a likelihood framework to correlate traits with accelerated evolution in amino acid sequences. "RER" also accounts for cases where a single branch contains the evolutionary signal by testing the significance of shifts in RERs both on the "single branch only" and on "all but this branch" for each respective foreground branch. We found a notable overlap where genes under accelerated evolution frequently exhibited positive selection. Among all endotherms, we found 479 genes (380 genes with evolutionary signals driven by multiple branches) showing significantly faster or slower evolutionary rates. Notably, *ddx54*, critical in genotoxic stress response and stimuli reception, displayed the highest relative rates among PSGs in S1. Among regional endotherms, we identified 517 genes (324 genes with evolutionary signals driven by multiple branches) with significant evolutionary rate shifts. The gene *pyroxd2*, involved in essential oxidoreductase processes for energy metabolism, exhibited the highest rate of evolution among PSGs in regional endotherms like tunas and sharks (S2). In eye/brain endotherms, 232 genes (100 genes with evolutionary signals driven by multiple branches) showed significant evolutionary rate shifts with *elapor1*, associated with cellular stress responses, having the highest rate of evolution (S3). In full-body endotherms (S4), 383 genes (208 genes with evolutionary signals driven by multiple branches) experienced significant rate variation. Here, *pdlim7*, crucial for the structural assembly of skeletal muscle, showed the highest evolutionary rate among PSGs (S4).

Our findings highlighted convergent evolution in PSGs like *carnmt1* and *dcaf6*, consistently selected across different nonoverlapping scenarios for their roles in muscle function and regulatory pathways. These results underscore shared genetic strategies for the evolution of endothermy, focusing on adaptations in muscle function and metabolic processes (Fig. 4E, figs. S13 to S18, and tables S18 to S26). However, only five (*ryr1*, *aco2*, *ephb2*, *mt-nd2*, and *pyroxd2*) (*1*, *4*, *25*–*27*) of the previously identified candidate genes for endothermy were confirmed under our more stringent analysis conditions. This illustrates the complexity and specificity of genetic adaptations for endothermy, suggesting that, although genes with convergent accelerated evolutionary rates do not always align with positive selection signals, their elevated rates may reflect unique, scenario-specific phenotypes (*63*) rather than direct contributions to endothermy. Our approach, emphasizing genes with both convergent evolutionary rates and positive selection, provides a robust framework for understanding the genetic basis of endothermy in marine vertebrates. Future research exploring gene duplications, losses, and regulatory or noncoding regions could offer deeper insights into the evolutionary mechanisms that enable these species to maintain higher body temperatures.

DISCUSSION

Building on an extensive dataset that includes a larger number of species and factors than previous studies (*1*, *4*, *5*, *12*, *17*), our analyses shed light on the evolutionary pathways of endothermy in marine vertebrates, particularly in ray-finned fishes. We integrated a comprehensive phylogenomic dataset of 1051 species with detailed ecological, morphological, and paleontological data alongside comparative genomic analyses of 205 genomes. We find that endothermy in ray-finned fishes arose in conjunction with a combination of body shape, specialized swimming, and ecological interactions with cetaceans during the Eocene-Miocene, rather than from climatic shifts or thermal expansion (*64*). Phylogenetic comparative analyses indicate strong correlations between endothermy and distinct morphologies, such as streamlined or deep-bodied forms, which vary across lineages and support high-performance swimming while rejecting links to depth range expansion (*7*) or dietary specialization. Although these findings represent correlations, our analyses suggest that the evolution of endothermy in ray-finned fishes was shaped by a complex interplay of ecological (e.g., swimming performance), morphological (e.g., body length and width), and genetic factors (Fig. 4). When considered alongside paleogeographic overlap with cetaceans (Fig. 3), the correlation with cetacean diversification supports that ecological interactions contributed to the evolution of endothermy, although these trends may also reflect shared responses to broader environmental pressures beyond the scope of our study. Endothermy in ray-finned fishes also exhibits substantial anatomical and physiological diversity, including full-body, regional, and eye/brain-specific endothermy. The ecological and locomotor benefits associated with endothermy likely vary across lineages depending on the form and extent of heat production. However, given the limited number of independent evolutionary origins for each type of endothermy, treating it as a generalized trait was necessary for robust phylogenetic comparative analyses. We separately distinguished endothermy types in our genomic comparisons (Fig. 4) to account for this biological variation. These considerations highlight that the selective pressures and functional outcomes associated with endothermy likely varied across lineages and may have included, but were not limited to, ecological interactions with cetaceans.

Endothermy's restricted distribution suggests evolutionary constraints akin to echolocation in bats and dolphins (*65*) or flight loss in birds (*66*). Our results suggest that endothermy in ray-finned fishes may have arisen in response to increased energetic demands driven by emerging ecological interactions with cetaceans in the marine realm. Endothermy represents an advanced physiological adaptation that emerged in lineages exhibiting ecomorphological traits common among pelagic fishes (*67*, *68*). Explaining why endothermy remains confined to certain lineages requires considering multiple factors: the high energetic cost of maintaining elevated body temperatures, ecological and functional trade-offs, genetic preadaptations, and phylogenetic constraints that may limit its evolution outside of certain ancestral conditions. For example, one or more of these factors could explain why the louvar, despite having internalized red muscle and a pelagic fast-swimming lifestyle similar to tunas, has not evolved endothermy (*69*). Although our findings reveal a correlation between the emergence of endothermy in ray-finned fishes and the evolutionary trends of modern cetaceans, the timing of its evolution across endothermic lineages suggests additional complex dynamics, particularly in older lineages of endothermic fishes. When considered alongside correlations with swimming mode, body morphology, and paleogeographic overlap with cetaceans, our results suggest that cetacean diversification and their ecological interactions with endothermic ray-finned fishes was likely a contributing factor to the evolution of endothermy rather than solely the emergence of faster prey.

The independent evolution of endothermy in chondrichthyans prior to the radiation of marine mammals suggests multiple selective pressures contributed to this trait. Ecological interactions like predation, niche differentiation, and prey capture were key drivers of gigantism and thermoregulation in large chondrichthyans (*14*). Competition with extinct apex predators, such as Mosasaurs and Megalodon, provides further parallels to dynamics in ray-finned fishes and cetaceans. Although a predator-prey arms race is a plausible evolutionary mechanism, this scenario alone is insufficient to explain the evolution of endothermy in ray-finned fishes as widespread convergence in swimming performance across distantly related prey groups, including small fishes, planktonic organisms, cephalopods, and crustaceans (*22*, *23*), would be required. Instead, our analyses show a temporal correlation between cetacean diversification and fish endothermy (Table 2), supporting an ecological interaction adaptation model. Benton (*19*) proposed that a competitive evolutionary arms race between synapsids and archosaurs during the Triassic led to the evolution of endothermy, not necessarily prey interactions. A similar dynamic may have occurred in marine ecosystems, where competition between predatory cetaceans and ray-finned fishes, rather than solely predator-prey interactions, exerted selective pressure favoring endothermy. Although we acknowledge that selective pressures to capture faster prey could have played a role, testing or falsifying this hypothesis would require a different framework to analyze independent prey adaptations across multiple lineages.

Comparative genomic analyses revealed convergent molecular adaptations for endothermy, with PSGs involved in metabolism, muscle function, and neural responses following similar evolutionary trajectories. Across multiple evolutionary scenarios, we identified shared genetic strategies, particularly among genes linked to energy metabolism and muscle function. Genes such as *carnmt1* and *dcaf6* show selection despite phylogenetic divergence, whereas *pyroxd2*, *elapor1*, and *pdlim7* exhibit scenario-specific adaptations in regional, eye/brain, and full-body endotherms, respectively. Distinct endothermy types exhibit scenario-specific genetic adaptations: *pyroxd2* evolves rapidly in tunas and sharks (regional endotherms), *elapor1* is associated with cellular stress responses in billfishes and marlins (eye/brain endotherms), and *pdlim7* facilitates muscle adaptation in full-body endotherms like marine mammals, opahs, and penguins. These findings highlight how molecular modifications enhance metabolic resilience across independent origins of endothermy. Although our focus was on convergent selection, future studies examining nonconvergent patterns could reveal lineage-specific adaptations and alternative evolutionary pathways to endothermy. The overlap between genes under positive selection and those with accelerated evolutionary rates underscores convergent pressures on metabolic and muscular pathways, although the limited confirmation of previously proposed candidate genes suggests a more complex genetic basis. Expanding taxonomic sampling, integrating experimental studies on functional development, and investigating the regulatory elements shaping endothermy through chromosome-level genome assemblies will be critical next steps in refining our understanding of vertebrate physiological adaptations. This work lays the foundation for future research into the genetic and ecological factors fueling complex trait evolution across taxa, enhancing our understanding of the evolution of unique traits.

MATERIALS AND METHODS

Sample collection and taxon selection

Our study used two datasets encompassing all major lineages of marine vertebrates that have independently evolved endothermy. The ray-finned fish dataset (RFFD) (table S1) included 1051 species for phylogenetic analysis. The marine vertebrate dataset (MVD) (table S17) comprised whole-genome sequencing data from 205 species used for comparative genomic analyses. The RFFD encompasses 1051 species and 1099 nuclear exon markers (table S1), with additionally sequenced genomic data for 763 species (dataset S1). It includes 22 endothermic teleosts from families such as Lampridae, Xiphiidae, and Scombridae. DNA samples were collected from voucher specimens across various museums (table S1). DNA extractions for 763 species of ray-finned fishes were sent to Arbor Biosciences for library preparation and target enrichment using the FishLife project exon probe sets (Backbone 2, Eupercaria, and Pelagiaria) (*70*). The RFFD was expanded using previously published data for an additional 285 species (*30*, *71*) and three outgroups, totaling 1051 species. The MVD contains whole-genome sequences from 205 marine species (table S17), including 138 long-read genomes from NCBI, 69 additional short-read genomes of ray-finned fishes (dataset S9), and a diverse range of taxa such as whales, seals, penguins, marine reptiles, and both ectothermic and endothermic ray-finned fishes. DNA for the short-read genomes was extracted and processed for sequencing at the Oklahoma Medical Research Foundation Clinical Genomics Center. Assemblies were obtained with coverage between 12X and 300X; in some cases, multiple individuals per species were sequenced.

Data assembly and quality control

Data assembly for the RFFD followed the Hughes *et al.* (*70*) bioinformatic pipeline. It eliminated low-quality bases and any traces of adapter contamination using Trimmomatic v0.36 (*72*). Mapping of the raw reads to the respective reference sequence was based on the three different Fishlife probe sets, using BioPython (*73*), the Burrows-Wheeler Alignment (BWA) tool (*74*), and SAMtools v.1.7-1.9 (*75*). Our initial assemblies were created using Velvet v1.2.10 (*76*). We used the automated target-restricted assembly method (aTRAM) software (*77*) with Trinity v2.8.5 (*78*) as the assembler. Reading frames were condensed and generated using CD-HIT (*79*) and exonerate (*80*). The assemblies were combined with previously published sequence data (*30*, *71*) and aligned using the Multiple Alignment of Coding Sequences MACSE v2.05 (*81*). We removed any instance of single-taxon insertions, trimmed gappy edges, and filtered short sequences using a custom Python script (Supplementary Text). We manually inspected ~20% of the gene alignments to check for reading frame modifications, potential misalignment, and data vetting using Geneious Prime v2022.2.2.

Two methods were used for comparative genomic data assembly for the 205 marine vertebrate species (MVD). Initially, a phylogenetic framework was constructed from 1099 (*70*) single-copy nuclear loci using the NHMMER tool within HMMER v3.1 (*82*). Assembly was conducted in Trinity v2.8.5 (*78*), and all mined sequences were aligned in MACSE v2.05 (*81*). The second method involved creating a probe set for 61 candidate genes related to endothermy obtained through an extensive literature review (*1*, *4*, *25*–*27*, *83*, *84*) (dataset S10) and sourcing the orthologs from the Ensembl genome browser. From our genomic dataset, 22 species with annotated genomes in

NCBI were chosen to find additional single-copy orthologous sequences. This process involved downloading genome annotations from NCBI and identifying 833 single-copy orthologous amino acid sequences using OrthoFinder v2.5.4 (*85*). A custom Python script (dataset S11) was then used to match these amino acid sequences with their corresponding nucleotide sequences in our reference genome. These 833 nucleotide sequences served as baits to extract sequences for the other 183 unannotated species (dataset S9), completing our collection of single-copy orthologs.

Phylogenomic analyses and divergence time estimation

Phylogenetic analyses for the RFFD and MVD datasets were performed using maximum likelihood (ML) and multispecies coalescent methods. Gene alignments were combined into a supermatrix with AMAS (*86*) (datasets S1 and S10), and preliminary trees were created using FastTree2 (*87*) for quality control (Supplementary Text). The best ML trees were derived using IQTREE v2.0 (*88*) under a "MIX" model (dataset S2); this approach is less computationally demanding than alternative techniques in determining the most suitable partitioning scheme for datasets (*71*, *89*). We estimated branch support on all ML datasets using the ultrafast bootstrapping approach with the "-bnni" argument on 1000 replicates (*88*). Gene trees were estimated from single-gene alignments using IQ-TREE and MIX models. The trees were pruned for bootstrap support below 30%. Last, species-tree analyses were completed with ASTRAL-III v5.1.1 (*90*) (dataset S2).

In our RFFD analysis, we addressed phylogenetic uncertainty by creating four genomic subsets, each containing around 220 loci and seven shared "anchor" legacy nuclear markers (*37*, *41*). We used IQTREE v2.0 for phylogenetic estimations on these subsets. Although multispecies coalescent methods are typically resilient to low and moderate missing data levels (*91*), we refrained from applying these methods to subsets where missing data exceeded 90%. This decision was made due to the substantial increase in gene tree errors associated with large amounts of missing data, a challenge for existing coalescent methods (*91*, *92*).

Divergence time estimation was performed only for the RFFD. Considering the computational challenges associated with estimating divergence times for large phylogenies within a Bayesian framework (*93*–*97*), we used a previously proposed MCMC (Markov chain Monte Carlo) time-calibrated tree of ray-finned fishes (*30*), which includes 303 species, as our reference tree. We used a congruification approach using geiger v.2.0 (*98*) and treePL (*99*). To account for uncertainty in divergence time, we used the three alternative calibration schemes presented by Hughes *et al.* (*30*) (datasets S2 to S6). We conducted an extensive comparison of our divergence times against other recently published time-calibrated phylogenies of ray-finned fishes at the family, order, and series level (*30*, *32*–*40*). Owing to the recent evidence of additional fossil species informing the time of evolution of Pelagiaria (*38*), Carangaria (*36*), Anabantaria (*36*), and Syngnatharia (*37*), we included eight additional fossil calibrations (table S2 and dataset S6) in our treePL analyses.

Compilation of ecological and morphological traits

We constructed an ecomorphological dataset for 1051 ray-finned fish species, incorporating five ecological traits that were hypothesized to influence the evolution of endothermy in fishes: average standard length (cm), length-weight relationship (g), swimming mode, diet, and depth range (m) (*1*, *4*, *13*, *17*, *84*, *100*, *101*) (table S3). The data for these traits were gathered from a variety of sources (*102*–*108*) (Supplementary Text). Dietary categories were extensively classified into 30 distinct groups, and swimming modes were differentiated into 11 unique types (Supplementary Text). This detailed categorization allowed for a nuanced analysis of the ecological factors contributing to endothermy, with the integrity of the data further ensured through cross-referencing and validation against multiple databases.

We leveraged the FS database (*46*) to examine the relationship between endothermy and various morphometric variables. This included average body depth (cm), average body width (cm), average head depth (cm), average mouth width corrected for size (cm), average caudal peduncle width (cm), average weight (g), body depth-length ratio (cm), and body depth-length-weight ratio (cm^2/g). Morphometric factors were calculated using formulas, such as the body depth-length ratio [(standard length/body depth) x standard length] and the body depth-length-weight ratio [(standard length/body depth) x weight]. To assess the robustness of our findings, we reassessed the average standard length using FS values, ensuring consistency with the data obtained from the various sources.

Correlated trait evolutionary analyses

To elucidate potential evolutionary correlations between the presence and absence of endothermy and its relationships to either multistate discrete characters (such as diet and swimming mode) or continuous characters (like average length, length/weight relationship, and depth range), we used a PGLR analysis (*48*) (Supplementary Text). We used the "phyloglm" function from the phylolm (*109*) R package to implement this model. Analyses were structured into univariate and multivariate frameworks for each factor with 1000 bootstrap replicates across all our estimated chronograms (19 total trees). The univariate approach explored the interaction between individual factors, whereas the multiple logistic regression frameworks incorporated interactions among all investigated factors (table S3) and endothermy. Given the inherent challenges in designating swimming modes to istiophorids, especially when differentiating between sub-carangiform and thunniform classifications (*1*, *17*, *110*–*112*), we conducted additional regressions for each proposed swimming mode (tables S5 to S8).

Ancestral reconstructions of endothermy

We used SIMMAP (*42*) to estimate ancestral character states for the presence or absence of endothermy for all of the most recent common ancestors (MRCA) in our RFFD phylogeny (*42*, *113*). We first assessed whether these transitions fit a model where shifts between state 0 and state 1, and vice versa, exhibit equal rates (ER) or if, instead, these transitions are different (ARD) (*114*). We performed stochastic character mapping (100 simulations) based on the best-fit model across our 19 total trees using the "make. simmap" command to account for phylogenetic and divergence time uncertainty in phytools v2.2-1 (*114*).

State-dependent diversification

Models for state-dependent speciation and extinction (SSE) (*115*) have proven to be a robust toolkit for inferring the processes that dictate the patterns of species richness and trait diversity (*45*, *116*), given that they jointly account for speciation (birth) and extinction (death) rates for each character of interest alongside state transition rates (*45*, *117*). By categorizing species into ectothermic "0" and endothermic "1" states, we used the hisse (*43*) package in R to evaluate

the evolutionary consequences of endothermy on diversification (dataset S6). The analysis included a range of SSE models, from the null BiSSE model, which assumes uniform birth and death rates across states (*118*), to the full BiSSE and HiSSE models, which allow for variable rates tied to the presence or absence of the trait. In addition, we explored endothermy-independent models based on two and four hidden states to ensure a comprehensive examination of diversification patterns. To address sampling biases due to the disproportionate representation of endothermic and ectothermic species, we adjusted our sampling fractions and conducted additional analyses with balanced proportions (Supplementary Text). The AIC guided our selection of the best-fit model, whereas a phylogenetic analysis of variance (ANOVA) in RRPP with Bonferroni correction (dataset S6) (*119*, *120*) was used to statistically compare diversification rates between states (Supplementary Text).

Model to assess time-variable associations in the origin of discrete traits

Studies have shown that climatic events have promoted many evolutionary tendencies (*6*, *13*). Although the potential impact that past climatic changes may have on the evolution of endothermy has been alluded to (*6*, *7*, *13*, *26*), no empirical methods exist to test this hypothesis across species. To account for these effects, we developed a modified time-dependent threshold model for binary characters on phylogenetic trees based on Felsenstein's threshold model (*50*), building on a likelihood approximation with numerical integration and quadratures using the general algorithm described in a previous study (*121*). This model assumes that the evolution of a binary trait is controlled by an unobserved (latent) continuous process (for instance, Brownian motion) controlling the transitions from one character state to another upon a given threshold. We rigorously tested the accuracy of our model with extensive simulations focusing on accurately detecting the generating model and inferring a relationship with climatic changes (Supplementary Text). We assigned character states based on the presence or absence of endothermy for each taxon. We conducted a model selection analysis in which we compared the fit of our modified climactic threshold model to other threshold models based on alternative latent processes like Brownian motion, Ornstein-Uhlenbeck, Early Burst, and Pagel's Lambda (Supplementary Text). To account for uncertainty, we ran our model selection analyses using all of our previously estimated phylogenies and divergence times and a variety of climatic curves (Supplementary Text).

Tests of biotic interactions in the origin of endothermy

To test for an evolutionary relationship between the emergence of endothermy in ray-finned fishes and the appearance of modern cetaceans in the ocean, we used our generalized threshold model mentioned above with a curve of group diversity. Using previously published tip-dated phylogenies for the whole cetacean group combined and Mysticeti and Odontoceti individually (*51*), we generated LTT curves as proxies of diversity for each group using the "ltt" function found in the phytools R package (*114*). We then refitted our threshold model by substituting the paleoclimatic curve with the estimated LTT curve. We accounted for the lack of extinction consideration when estimating LTTs using only extant species by using tip-dated phylogenies. We also calculated the DTT for the cetaceans (Supplementary Text). Because DTT estimation is based on an ultrametric tree, we estimated DTT values for all extant cetaceans (Odontoceti + Mysticeti) combined (*51*) but avoided doing separate analyses for the Odontoceti and Mysticeti groups, respectively, because, when removing the fossil tips, the remaining taxonomic sampling was low (<100 species), which can compromise the accuracy of our model (figs. S1 to S7). In addition, we estimated the LTT and DTT values for all elasmobranchs using a previously published phylogeny (*53*). Although the elasmobranch phylogeny by Stein *et al.* (*53*) is one of the most taxonomically well-sampled ones, it lacks fossils as terminal taxa, risking biased LTT results. Although using DTT values helps account for these potential issues, we also conducted additional analyses using LTT values for a tip-dated phylogeny of Carchariniformes and DTT estimates (*54*) (Supplementary Text). Our modified threshold model was tested against various artificially adjusted dates that altered the origin of endothermy by 50 and 25%, respectively, to further validate our results and avoid any potential instance of a false positive. Running this model with artificially older origins for endothermy resulted in failed convergence runs because most transitions were pushed beyond the appearance of cetacean lineages.

Tests of positive selection, rates of evolution, and molecular convergence

Our study examined 894 single-copy orthologs to identify selection patterns within the MVD, which encompasses 205 species (table S17 and datasets S8 and S9). We used two modified versions of the BUSTED analysis from the HyPhy package (*58*): BUSTED-E and BUSTED-PH, both extensions of the BUSTED[S] model that consider rate variations across synonymous sites (SRV) (*59*, *60*). BUSTED-E specifically filters alignment errors by isolating problematic sequence regions into an error-sink category, ensuring that they do not skew the overall ω distribution used to detect selection (Supplementary Text).

BUSTED-PH is designed to detect signals of positive selection that are associated with a particular binary phenotype, distinguishing between phylogeny-wide positive selection and selection in genes evolving convergently (*60*). The model uses an unrestricted dN/dS distribution and three distinct null models to discern foreground-specific positive selection, background-specific positive selection, and differences between foreground and background branches. For positive selection tests, the null model constrains dN/dS to be at most 1 for either the foreground or background branches, whereas the other branches are left unconstrained, and for differences between branches, it fits a single tree-wide unrestricted dN/dS distribution. This approach allows us to categorize signatures of selection based on their association with the selection being observed (Supplementary Text). BUSTED-PH introduces a third "nuisance" branch category, which is not directly involved in the inference process (*60*). This feature was instrumental in our study as it allowed us to categorize the selection signals by comparing endotherms against ectotherms in different scenarios: endotherms (fg) versus ectotherms (bg), regional endotherms (fg) versus ectotherms (bg), eye/brain endotherms (fg) versus ectotherms (bg), and full-body endotherms (fg) versus ectotherms (bg) (Supplementary Text). This feature helped clarify how each type of endothermy contributes to the selection signals detected. Crucially, BUSTED-PH preserves the integrity of our taxonomic sampling, avoiding the pitfalls of other methods that might inadvertently increase the risk of false positives by pruning "nuisance" species (*60*).

Our experiment used the Protein Analysis Through Evolutionary Relationships (PANTHER) database to classify the functions of the genes we identified (*61*). It organizes genes into families and

subfamilies, creating a structured framework that facilitates the visualization and summarization of each gene's role (*61*). This systematic categorization allowed us to make efficient functional comparisons, substantially broadening our comprehension of how these genes contribute to the trait of endothermy in marine vertebrates. We also looked at the relative rates of evolution for each gene. This was achieved using the "RER" functionality in Hyphy, which evaluates the correlation between the rate of gene evolution and the trait of interest, in this case, endothermy (*62*, *63*). By incorporating this approach, we added an additional layer to our phenotype-to-genotype association analysis, allowing us to not only focus on genes under positive selection but also consider those evolving at the most rapid rates. These analyses provided additional evidence supporting the convergence signals we observed in endothermic species.

Supplementary Materials

This PDF file includes:

Supplementary Text
Figs. S1 to S18
Legends for tables S1 to S27
Legends for datasets S1 to S11
References

REFERENCES AND NOTES

1. B. A. Block, J. R. Finnerty, Endothermy in fishes: A phylogenetic analysis of constraints, predispositions, and selection pressures. *Environ. Biol. Fishes* **40**, 283–302 (1994).
2. W. J. Hillenius, J. A. Ruben, The evolution of endothermy in terrestrial vertebrates: Who? When? Why? *Physiol. Biochem. Zool.* **77**, 1019–1042 (2004).
3. L. J. Legendre, D. Davesne, The evolution of mechanisms involved in vertebrate endothermy. *Philos. Trans. R. Soc. London Ser. B Biol. Sci.* **375**, 20190136 (2020).
4. K. A. Dickson, J. B. Graham, Evolution and consequences of endothermy in fishes. *Physiol. Biochem. Zool.* **77**, 998–1018 (2004).
5. D. J. Madigan, A. B. Carlisle, L. D. Gardner, N. Jayasundara, F. Micheli, K. M. Schaefer, D. W. Fuller, B. A. Block, Assessing niche width of endothermic fish from genes to ecosystem. *Proc. Natl. Acad. Sci. U.S.A.* **112**, 8350–8355 (2015).
6. J. Rolland, D. Silvestro, D. Schluter, A. Guisan, O. Broennimann, N. Salamin, The impact of endothermy on the climatic niche evolution and the distribution of vertebrate diversity. *Nat. Ecol. Evol.* **2**, 459–464 (2018).
7. L. Harding, A. Jackson, A. Barnett, I. Donohue, L. Halsey, C. Huveneers, C. Meyer, Y. Papastamatiou, J. M. Semmens, E. Spencer, Y. Watanabe, N. Payne, Endothermy makes fishes faster but does not expand their thermal niche. *Funct. Ecol.* **35**, 1951–1959 (2021).
8. D. Bernal, K. A. Dickson, R. E. Shadwick, J. B. Graham, Review: Analysis of the evolutionary convergence for high-performance swimming in lamnid sharks and tunas. *Comp. Biochem. Physiol. A Mol. Integr. Physiol.* **129**, 695–726 (2001).
9. B. A. Block, J. R. Finnerty, A. F. Stewart, J. Kidd, Evolution of endothermy in fish: Mapping physiological traits on a molecular phylogeny. *Science* **260**, 210–214 (1993).
10. F. G. Carey, K. D. Lawson, Temperature regulation in free-swimming bluefin tuna. *Comp. Biochem. Physiol. A Comp. Physiol.* **44**, 375–392 (1973).
11. K. A. Dickson, N. M. Johnson, J. M. Donley, J. A. Hoskinson, M. W. Hansen, J. D'souza Tessier, Ontogenetic changes in characteristics required for endothermy in juvenile black skipjack tuna (*Euthynnus lineatus*). *J. Exp. Biol.* **203**, 3077–3087 (2000).
12. J. B. Thiebot, J. C. McInnes, Why do marine endotherms eat gelatinous prey? *ICES J. Mar. Sci.* **77**, 58–71 (2020).
13. H. G. Ferrón, Regional endothermy as a trigger for gigantism in some extinct macropredatory sharks. *PLOS ONE* **12**, e0185185 (2017).
14. C. Pimiento, J. L. Cantalapiedra, K. Shimada, D. J. Field, J. B. Smaers, Evolutionary pathways toward gigantism in sharks and rays. *Evolution* **73**, 588–599 (2019).
15. R. W. Brill, Selective advantages conferred by the high-performance physiology of tunas, billfishes, and dolphin fish. *Comp. Biochem. Physiol. A Mol. Integr. Physiol.* **113**, 3–15 (1996).
16. J. B. Graham, K. A. Dickson, The evolution of thunniform locomotion and heat conservation in scombrid fishes: New insights based on the morphology of *Allothunnus fallai*. *Zool. J. Linn. Soc.* **129**, 419–466 (2000).
17. Y. Y. Watanabe, K. J. Goldman, J. E. Caselle, D. D. Chapman, Y. P. Papastamatiou, Comparative analyses of animal-tracking data reveal ecological significance of endothermy in fishes. *Proc. Natl. Acad. Sci. U.S.A.* **112**, 6104–6109 (2015).
18. V. Domínguez-García, S. Kéfi, The structure and robustness of ecological networks with two interaction types. *PLoS Comput. Biol.* **20**, e1011770 (2024).
19. M. J. Benton, The origin of endothermy in synapsids and archosaurs and arms races in the Triassic. *Gondw. Res.* **100**, 261–289 (2021).
20. K. A. Monsch, A revision of scombrid fishes (*Scombroidei, Perciformes*) from the Middle Eocene of Monte Bolca, Italy. *Palaeontology* **49**, 873–888 (2006).
21. F. Santini, G. Carnevale, L. Sorenson, First molecular scombrid timetree (*Percomorpha: Scombridae*) shows recent radiation of tunas following invasion of pelagic habitat. *Ital. J. Zool.* **80**, 210–221 (2013).
22. M. B. Santos, G. J. Pierce, Cetacean diet. *Encycl. Anim. Cogn. Behav.* **1**, 1–9 (2017).
23. M. S. Savoca, M. F. Czapanskiy, S. R. Kahane-Rapport, W. T. Gough, J. A. Fahlbusch, K. C. Bierlich, P. S. Segre, J. Di Clemente, G. S. Penry, D. N. Wiley, J. Calambokidis, D. P. Nowacek, D. W. Johnston, N. D. Pyenson, A. S. Friedlaender, E. L. Hazen, J. A. Goldbogen, Baleen whale prey consumption based on high-resolution foraging measurements. *Nature* **599**, 85–90 (2021).
24. R. Motani, K. Shimada, Skeletal convergence in thunniform sharks, ichthyosaurs, whales, and tunas, and its possible ecological links through marine ecosystem evolution. *Sci. Rep.* **13**, 16664 (2023).
25. B. Wu, C. Feng, C. Zhu, W. Xu, Y. Yuan, M. Hu, K. Yuan, Y. Li, Y. Ren, Y. Zhou, H. Jiang, Q. Qiu, W. Wang, S. He, K. Wang, The genomes of two billfishes provide insights into the evolution of endothermy in teleosts. *Mol. Biol. Evol.* **19**, 2413–2427 (2021).
26. A. G. Ciezarek, O. G. Osborne, O. N. Shipley, E. J. Brooks, S. R. Tracey, J. D. McAllister, L. D. Gardner, M. J. E. Sternberg, B. Block, V. Savolainen, Phylotranscriptomic insights into the diversification of endothermic *Thunnus* tunas. *Mol. Biol. Evol.* **36**, 84–96 (2019).
27. X. Wang, M. Qu, Y. Liu, R. F. Schneider, Y. Song, Z. Chen, H. Zhang, Y. Zhang, H. Yu, S. Zhang, D. Li, G. Qin, S. Ma, J. Zhong, J. Yin, S. Liu, G. Fan, A. Meyer, D. Wang, Q. Lin, Genomic basis of evolutionary adaptation in a warm-blooded fish. *Innovation* **3**, 100185 (2022).
28. J. Bo, W. Q. Lv, N. Sun, C. Wang, K. Wang, P. Liu, C. G. Feng, S. P. He, L. D. Yang, Opah (*Lampris megalopsis*) genome sheds light on the evolution of aquatic endothermy. *Zool. Res.* **43**, 26–29 (2022).
29. B. T. L. Nichio, J. N. Marchaukoski, R. T. Raittz, New tools in orthology analysis: A brief review of promising perspectives. *Front. Genet.* **8**, 165 (2017).
30. L. C. Hughes, G. Ortí, Y. Huang, Y. Sun, C. C. Baldwin, A. W. Thompson, D. Arcila, R. Betancur-R, C. Li, L. Becker, N. Bellora, X. Zhao, X. Li, M. Wang, C. Fang, B. Xie, Z. Zhou, H. Huang, S. Chen, B. Venkatesh, Q. Shi, Comprehensive phylogeny of ray-finned fishes (*Actinopterygii*) based on transcriptomic and genomic data. *Proc. Natl. Acad. Sci. U.S.A.* **115**, 6249–6254 (2018).
31. J. M. Eastman, L. J. Harmon, D. C. Tank, Congruification: Support for time scaling large phylogenetic trees. *Methods Ecol. Evol.* **4**, 688–691 (2013).
32. R. Betancur-R, E. O. Wiley, G. Arratia, A. Acero, N. Bailly, M. Miya, G. Lecointre, G. Ortí, Phylogenetic classification of bony fishes. *BMC Evol. Biol.* **17**, 162 (2017).
33. T. J. Near, R. I. Eytan, A. Dornburg, K. L. Kuhn, J. A. Moore, M. P. Davis, P. C. Wainwright, M. Friedman, W. L. Smith, Resolution of ray-finned fish phylogeny and timing of diversification. *Proc. Natl. Acad. Sci. U.S.A.* **109**, 13698–13703 (2012).
34. D. L. Rabosky, J. Chang, P. O. Title, P. F. Cowman, L. Sallan, M. Friedman, K. Kaschner, C. Garilao, T. J. Near, M. Coll, M. E. Alfaro, An inverse latitudinal gradient in speciation rate for marine fishes. *Nature* **559**, 392–395 (2018).
35. M. E. Alfaro, B. C. Faircloth, R. C. Harrington, L. Sorenson, M. Friedman, C. E. Thacker, C. H. Oliveros, D. Černý, T. J. Near, Explosive diversification of marine fishes at the Cretaceous–Palaeogene boundary. *Nat. Ecol. Evol.* **2**, 688–696 (2018).
36. E. Ribeiro, A. M. Davis, R. A. Rivero-Vega, G. Ortí, R. Betancur-R, Post-Cretaceous bursts of evolution along the benthic-pelagic axis in marine fishes. *Proc. Biol. Sci.* **285**, 20182010 (2018).
37. A. Santaquiteria, A. C. Siqueira, E. Duarte-Ribeiro, G. Carnevale, W. T. White, J. J. Pogonoski, C. C. Baldwin, G. Ortí, D. Arcila, B. R. Ricardo, Phylogenomics and historical biogeography of seahorses, dragonets, goatfishes, and allies (*Teleostei: Syngnatharia*): Assessing factors driving uncertainty in biogeographic inferences. *Syst. Biol.* **70**, 1145–1162 (2021).
38. M. Friedman, K. L. Feilich, H. T. Beckett, M. E. Alfaro, B. C. Faircloth, D. Černý, M. Miya, T. J. Near, R. C. Harrington, A phylogenomic framework for pelagiarian fishes (*Acanthomorpha: Percomorpha*) highlights mosaic radiation in the open ocean. *Proc. R. Soc. London Ser. B Biol. Sci.* **286**, 20191502 (2019).
39. R. C. Harrington, B. C. Faircloth, R. I. Eytan, W. L. Smith, T. J. Near, M. E. Alfaro, M. Friedman, Phylogenomic analysis of carangimorph fishes reveals flatfish asymmetry arose in a blink of the evolutionary eye. *BMC Evol. Biol.* **16**, 224 (2016).
40. A. Ghezelayagh, R. C. Harrington, E. D. Burress, M. A. Campbell, J. C. Buckner, P. Chakrabarty, J. R. Glass, W. T. McCraney, P. J. Unmack, C. E. Thacker, M. E. Alfaro, S. T. Friedman, W. B. Ludt, P. F. Cowman, M. Friedman, S. A. Price, A. Dornburg, B. C. Faircloth, P. C. Wainwright, T. J. Near, Prolonged morphological expansion of spiny-rayed fishes following the end-Cretaceous. *Nat. Ecol. Evol.* **6**, 1211–1220 (2022).

41. M. Rincon-Sandoval, E. Duarte-Ribeiro, A. M. Davis, A. Santaquiteria, L. C. Hughes, C. C. Baldwin, L. Soto-Torres, A. P. Acero, H. J. Walker, K. E. Carpenter, M. Sheaves, G. Ortí, D. Arcila, R. R. Betancur-R, Evolutionary determinism and convergence associated with water-column transitions in marine fishes. *Proc. Natl. Acad. Sci. U.S.A.* **117**, 33396–33403 (2020).
42. J. P. Bollback, SIMMAP: Stochastic character mapping of discrete traits on phylogenies. *BMC Bioinformatics* **7**, 88 (2006).
43. J. M. Beaulieu, B. C. O'Meara, Detecting hidden diversification shifts in models of trait-dependent speciation and extinction. *Syst. Biol.* **65**, 583–601 (2016).
44. P. C. Wainwright, S. J. Longo, Functional innovations and the conquest of the oceans by acanthomorph fishes. *Curr. Biol.* **27**, R550–R557 (2017).
45. J. Ng, S. D. Smith, Why are red flowers so rare? Testing the macroevolutionary causes of tippiness. *J. Evol. Biol.* **31**, 1863–1875 (2018).
46. S. A. Price, S. T. Friedman, K. A. Corn, O. Larouche, K. Brockelsby, A. J. Lee, M. Nagaraj, N. G. Bertrand, M. Danao, M. C. Coyne, J. R. Estrada, R. Friedman, E. Hoeft, M. Iwan, D. Gross, J. H. Kao, B. Landry, M. J. Linares, C. McGlinn, J. A. Nguyen, A. G. Proffitt, S. Rodriguez, M. R. Rupp, E. Y. Shen, V. Susman, A. J. Tovar, L. L. J. Vary, K. L. Zapfe, P. C. Wainwright, FishShapes v1: Functionally relevant measurements of teleost shape and size on three dimensions. *Ecology* **103**, e3829 (2022).
47. V. Di Santo, E. Goerig, D. K. Wainwright, O. Akanyeti, J. C. Liao, T. Castro-Santos, G. V. Lauder, Convergence of undulatory swimming kinematics across a diversity of fishes. *Proc. Natl. Acad. Sci. U.S.A.* **118**, e2113206118 (2021).
48. A. R. Ives, T. Garland, Phylogenetic logistic regression for binary dependent variables. *Syst. Biol.* **59**, 9–26 (2010).
49. B. A. Block, Endothermy in fish: Thermogenesis, ecology, and evolution. *Biochem. Mol. Biol. Fishes* **1**, 269–311 (1991).
50. J. Felsenstein, D. D. Ackerly, M. A. McPeek, A comparative method for both discrete and continuous characters using the threshold model. *Am. Nat.* **179**, 145–156 (2012).
51. G. Burin, T. Park, T. D. James, G. J. Slater, N. Cooper, The dynamic adaptive landscape of cetacean body size. *Curr. Biol.* **33**, 1787–1794.e3 (2023).
52. M. A. Silva, R. Feio, R. Prieto, J. M. Gonçalves, R. S. Santos, Interactions between cetaceans and the tuna fishery in the Azores. *Mar. Mamm. Sci.* **18**, 893–901 (2002).
53. R. W. Stein, C. G. Mull, T. S. Kuhn, N. C. Aschliman, L. N. K. Davidson, J. B. Joy, G. J. Smith, N. K. Dulvy, A. O. Mooers, Global priorities for conserving the evolutionary history of sharks, rays, and chimaeras. *Nat. Ecol. Evol.* **2**, 288–298 (2018).
54. B. Brée, F. L. Condamine, G. Guinot, Combining palaeontological and neontological data shows a delayed diversification burst of carcharhiniform sharks likely mediated by environmental change. *Sci. Rep.* **12**, 21906 (2022).
55. A. F. Bennett, J. A. Ruben, Endothermy and activity in vertebrates. *Science* **206**, 649–654 (1979).
56. L. J. Revell, L. J. Harmon, D. C. Collar, Phylogenetic signal, evolutionary process, and rate. *Syst. Biol.* **57**, 591–601 (2008).
57. A. Capobianco, M. Friedman, Vicariance and dispersal in southern hemisphere freshwater fish clades: A palaeontological perspective. *Biol. Rev. Camb. Philos. Soc.* **94**, 662–699 (2019).
58. S. L. Kosakovsky Pond, A. F. Y. Poon, R. Velazquez, S. Weaver, N. L. Hepler, B. Murrell, S. D. Shank, B. R. Magalis, D. Bouvier, A. Nekrutenko, S. Wisotsky, S. J. Spielman, S. D. W. Frost, S. V. Muse, HyPhy 2.5—A customizable platform for evolutionary hypothesis testing using phylogenies. *Mol. Biol. Evol.* **37**, 295–299 (2020).
59. S. R. Wisotsky, S. L. K. Pond, S. D. Shank, S. V. Muse, Synonymous site-to-site substitution rate variation dramatically inflates false positive rates of selection analyses: Ignore at your own peril. *Mol. Biol. Evol.* **37**, 2430–2439 (2020).
60. A. Selberg, N. L. Clark, T. B. Sackton, S. V. Muse, A. G. Lucaci, S. Weaver, A. Nekrutenko, M. Chikina, S. L. Kosakovsky Pond, Minus the error: Estimating dN/dS and testing for natural selection in the presence of residual alignment errors. bioRxiv 2024.11.13.620707 [Preprint] (2024). https://doi.org/10.1101/2024.11.13.620707.
61. P. D. Thomas, D. Ebert, A. Muruganujan, T. Mushayahama, L. P. Albou, H. Mi, PANTHER: Making genome-scale phylogenetics accessible to all. *Protein Sci.* **31**, 8–22 (2022).
62. A. Kowalczyk, W. K. Meyer, R. Partha, W. Mao, N. L. Clark, M. Chikina, RERconverge: An R package for associating evolutionary rates with convergent traits. *Bioinformatics* **35**, 4815–4817 (2019).
63. A. Kowalczyk, M. Chikina, N. L. Clark, Complementary evolution of coding and noncoding sequence underlies mammalian hairlessness. *Elife* **11**, e76911 (2022).
64. W. H. Neill, R. K. Chang, A. E. Dizon, Magnitude and ecological implications of thermal inertia in skipjack tuna, *Katsuwonus pelamis* (Linnaeus). *Environ. Biol. Fishes* **1**, 61–80 (1976).
65. J. Parker, G. Tsagkogeorga, J. A. Cotton, Y. Liu, P. Provero, P. Stupka, S. J. Rossiter, Genome-wide signatures of convergent evolution in echolocating mammals. *Nature* **502**, 228–231 (2013).
66. S. Pan, Y. Lin, Q. Liu, J. Duan, Z. Lin, Y. Wang, X. Wang, S. M. Lam, Z. Zou, G. Shui, Y. Zhang, Z. Zhang, X. Zhan, Convergent genomic signatures of flight loss in birds suggest a switch of main fuel. *Nat. Commun.* **10**, 2756 (2019).
67. F. Seebacher, Is endothermy an evolutionary by-product? *Trends Ecol. Evol.* **35**, 503–511 (2020).
68. N. L. Payne, E. P. Snelling, R. Fitzpatrick, J. Seymour, R. Courtney, A. Barnett, Y. Y. Watanabe, D. W. Sims, L. Squire, J. M. Semmens, A new method for resolving uncertainty of energy requirements in large water breathers: The 'mega-flume' seagoing swim-tunnel respirometer. *Methods Ecol. Evol.* **6**, 668–677 (2015).
69. M. C. Arostegui, M. R. Shero, L. R. Frank, R. M. Berquist, C. D. Braun, An enigmatic pelagic fish with internalized red muscle: A future regional endotherm or forever an ectotherm? *J. Fish Biol.* **102**, 1311–1326 (2023).
70. L. C. Hughes, G. Ortí, H. Saad, C. Li, W. T. White, C. C. Baldwin, K. A. Crandall, D. Arcila, R. Betancur-R, Exon probe sets and bioinformatics pipelines for all levels of fish phylogenomics. *Mol. Ecol. Resour.* **21**, 816–833 (2021).
71. D. Arcila, L. C. Hughes, F. Meléndez-Vázquez, C. C. Baldwin, W. T. White, K. E. Carpenter, J. T. Williams, M. D. Santos, J. J. Pogonoski, M. Miya, G. Ortí, R. Betancur-R, Testing the utility of alternative metrics of branch support to address the ancient evolutionary radiation of tunas, stromateoids, and allies (*Teleostei: Pelagiaria*). *Syst. Biol.* **70**, 1123–1144 (2021).
72. A. M. Bolger, M. Lohse, B. Usadel, Trimmomatic: A flexible trimmer for Illumina sequence data. *Bioinformatics* **30**, 2114–2120 (2014).
73. G. Van Rossum, F. L. Drake, *Python 3 Reference Manual* (CreateSpace, 2009).
74. H. Li, R. Durbin, Fast and accurate short-read alignment with Burrows–Wheeler transform. *Bioinformatics* **25**, 1754–1760 (2009).
75. P. Danecek, J. K. Bonfield, J. Liddle, J. Marshall, V. Ohan, M. O. Pollard, A. Whitwham, T. Keane, S. A. McCarthy, R. M. Davies, Twelve years of SAMtools and BCFtools. *Gigascience* **10**, giab008 (2021).
76. D. R. Zerbino, E. Birney, Velvet: Algorithms for de novo short read assembly using de Bruijn graphs. *Genome Res.* **18**, 821–829 (2008).
77. J. M. Allen, R. LaFrance, R. A. Folk, K. P. Johnson, R. P. Guralnick, aTRAM 2.0: An improved, flexible locus assembler for NGS data. *Evol. Bioinform. Online* **14**, 1176934318774546 (2018).
78. M. G. Grabherr, B. J. Haas, M. Yassour, J. Z. Levin, D. A. Thompson, I. Amit, X. Adiconis, L. Fan, R. Raychowdhury, Q. Zeng, Z. Chen, E. Mauceli, N. Hacohen, A. Gnirke, N. Rhind, F. Di Palma, B. W. Birren, C. Nusbaum, K. Lindblad-Toh, N. Friedman, A. Regev, Trinity: Reconstructing a full-length transcriptome without a genome from RNA-Seq data. *Nat. Biotechnol.* **29**, 644–652 (2011).
79. L. Fu, B. Niu, Z. Zhu, S. Wu, W. Li, CD-HIT: Accelerated for clustering the next-generation sequencing data. *Bioinformatics* **28**, 3150–3152 (2012).
80. G. S. C. Slater, E. Birney, Automated generation of heuristics for biological sequence comparison. *BMC Bioinformatics* **6**, 31 (2005).
81. V. Ranwez, E. J. P. Douzery, C. Cambon, N. Chantret, F. Delsuc, MACSE v2: Toolkit for the alignment of coding sequences accounting for frameshifts and stop codons. *Mol. Biol. Evol.* **35**, 2582–2584 (2018).
82. T. J. Wheeler, S. R. Eddy, Nhmmer: DNA homology search with profile HMMs. *Bioinformatics* **29**, 2487–2489 (2013).
83. G. L. J. Galli, M. S. Lipnick, H. A. Shiels, B. A. Block, Temperature effects on Ca^{2+} cycling in scombrid cardiomyocytes: A phylogenetic comparison. *J. Exp. Biol.* **214**, 1068–1076 (2011).
84. J. C. Patterson, C. A. Sepulveda, D. Bernal, The vascular morphology and in vivo muscle temperatures of thresher sharks (*Alopiidae*). *J. Morphol.* **272**, 1353–1364 (2011).
85. D. M. Emms, S. Kelly, OrthoFinder: Phylogenetic orthology inference for comparative genomics. *Genome Biol.* **20**, 238 (2019).
86. M. L. Borowiec, AMAS: A fast tool for alignment manipulation and computing of summary statistics. *PeerJ* **28**, e1600 (2016).
87. M. N. Price, P. S. Dehal, A. P. Arkin, FastTree 2—Approximately maximum-likelihood trees for large alignments. *PLOS ONE* **5**, e9490 (2010).
88. B. Q. Minh, H. A. Schmidt, O. Chernomor, D. Schrempf, M. D. Woodhams, A. Von Haeseler, R. Lanfear, E. Teeling, IQ-TREE 2: New models and efficient methods for phylogenetic inference in the genomic era. *Mol. Biol. Evol.* **37**, 1530–1534 (2020).
89. P. Kapli, Z. Yang, M. J. Telford, Phylogenetic tree building in the genomic age. *Nat. Rev. Genet.* **21**, 428–444 (2020).
90. C. Zhang, M. Rabiee, E. Sayyari, S. Mirarab, ASTRAL-III: Polynomial time species tree reconstruction from partially resolved gene trees. *BMC Bioinformatics* **19**, 153 (2018).
91. M. Nute, J. Chou, E. K. Molloy, T. Warnow, The performance of coalescent-based species tree estimation methods under models of missing data. *BMC Genomics* **19**, 286 (2018).
92. X. Jiao, T. Flouri, Z. Yang, Multispecies coalescent and its applications to infer species phylogenies and cross-species gene flow. *Natl. Sci. Rev.* **8**, nwab127 (2021).
93. T. Britton, C. L. Anderson, D. Jacquet, S. Lundqvist, K. Bremer, Estimating divergence times in large phylogenetic trees. *Syst. Biol.* **56**, 741–752 (2007).
94. R. A. Pyron, J. J. Wiens, A large-scale phylogeny of Amphibia including over 2800 species, and a revised classification of extant frogs, salamanders, and caecilians. *Mol. Phylogenet. Evol.* **61**, 543–583 (2011).

95. K. Tamura, F. U. Battistuzzi, P. Billing-Ross, O. Murillo, A. Filipski, S. Kumar, Estimating divergence times in large molecular phylogenies. *Proc. Natl. Acad. Sci. U.S.A.* **109**, 19333–19338 (2012).
96. S. A. Smith, J. M. Beaulieu, A. Stamatakis, M. J. Donoghue, Understanding angiosperm diversification using small and large phylogenetic trees. *Am. J. Bot.* **98**, 404–414 (2011).
97. C. E. Hinchliff, E. H. Roalson, Using supermatrices for phylogenetic inquiry: An example using the sedges. *Syst. Biol.* **62**, 205–219 (2013).
98. M. W. Pennell, J. M. Eastman, G. J. Slater, J. W. Brown, J. C. Uyeda, R. G. Fitzjohn, M. E. Alfaro, L. J. Harmon, geiger v2.0: An expanded suite of methods for fitting macroevolutionary models to phylogenetic trees. *Bioinformatics* **30**, 2216–2218 (2014).
99. S. A. Smith, B. C. O'Meara, treePL: Divergence time estimation using penalized likelihood for large phylogenies. *Bioinformatics* **28**, 2689–2690 (2012).
100. Y. Y. Watanabe, I. Nakamura, W. C. Chiang, Behavioural thermoregulation linked to foraging in blue sharks. *Mar. Biol.* **168**, 161 (2021).
101. A. Stoehr, J. St. Martin, S. Aalbers, C. Sepulveda, D. Bernal, Free-swimming swordfish, *Xiphias gladius*, alter the rate of whole-body heat transfer: Morphological and physiological specializations for thermoregulation. *ICES J. Mar. Sci.* **75**, 858–870 (2018).
102. R. Froese, D. Pauly, Fishbase (2023); https://fishbase.se/search.php.
103. D. R. Robertson, J. Van Tassell, Shorefishes of the Greater Caribbean: Online Information System (2023); https://biogeodb.stri.si.edu/caribbean/en/pages.
104. J. S. Nelson, T. C. Grande, M. V. H. Wilson, *Fish of the World* (Wiley, 2016), pp. 1–752.
105. Museums Victoria, Fishes of Australia, https://fishesofaustralia.net.au/ [accessed 2023].
106. FAO. FISHSTAT Database, https://fao.org/fishery/en/fishstat [accessed 2023].
107. J. Pickering, Discover Life Database, https://www.discoverlife.org/ [accessed 2023].
108. Reeflex, Fishes, https://reeflex.net/ [accessed 2023].
109. L. S. Tung Ho, C. Ané, A linear-time algorithm for Gaussian and non-Gaussian trait evolution models. *Syst. Biol.* **63**, 397–408 (2014).
110. G. J. Li, L. Zhu, X. Y. Lu, Numerical studies on locomotion performance of fish-like tail fins. *J. Hydrodynam.* **24**, 488–495 (2012).
111. D. H. Kühlmann, B. B. Collette, C. E. Nauen, *FAO Species Catalogue. Vol. 2, Scombrids of the World. FAO Fisheries Synopsis No. 125* (FAO, 1983), 137 pp.
112. R. W. Blake, L. M. Chatters, P. Domenici, Turning radius of yellowfin tuna (*Thunnus albacares*) in unsteady swimming manoeuvres. *J. Fish Biol.* **46**, 536–538 (1995).
113. A. Y. Hsiang, D. J. Field, T. H. Webster, A. D. B. Behlke, M. B. Davis, R. A. Racicot, J. A. Gauthier, The origin of snakes: Revealing the ecology, behavior, and evolutionary history of early snakes using genomics, phenomics, and the fossil record. *BMC Evol. Biol.* **15**, 87 (2015).
114. L. J. Revell, *phytools*: An R package for phylogenetic comparative biology (and other things). *Methods Ecol. Evol.* **3**, 217–223 (2012).
115. K. Magnuson-Ford, S. P. Otto, Linking the investigations of character evolution and species diversification. *Am. Nat.* **180**, 225–245 (2012).
116. R. G. Fitzjohn, Quantitative traits and diversification. *Syst. Biol.* **59**, 619–633 (2010).
117. J. Ng, S. D. Smith, How traits shape trees: New approaches for detecting character state-dependent lineage diversification. *J. Evol. Biol.* **27**, 2035–2045 (2014).
118. W. P. Maddison, P. E. Midford, S. P. Otto, Estimating a binary character's effect on speciation and extinction. *Syst. Biol.* **56**, 701–710 (2007).
119. M. L. Collyer, D. C. Adams, *RRPP*: An R package for fitting linear models to high-dimensional data using residual randomization. *Methods Ecol. Evol.* **9**, 1772–1779 (2018).
120. D. C. Adams, M. L. Collyer, Phylogenetic ANOVA: Group-clade aggregation, biological challenges, and a refined permutation procedure. *Evolution* **72**, 1204–1215 (2018).
121. G. Hiscott, C. Fox, M. Parry, D. Bryant, Efficient recycled algorithms for quantitative trait models on phylogenies. *Genome Biol. Evol.* **8**, 1338–1350 (2016).
122. H. Wickham, ggplot2. *Wiley Interdiscip. Rev. Comput. Stat.* **3**, 180–185 (2011).
123. E. M. Troyer, R. Betancur-R, L. C. Hughes, M. Westneat, G. Carnevale, W. T. White, J. J. Pogonoski, J. C. Tyler, C. C. Baldwin, G. Ortí, A. Brinkworth, J. Clavel, D. Arcila, The impact of paleoclimatic changes on body size evolution in marine fishes. *Proc. Natl. Acad. Sci. U.S.A.* **119**, e2122486119 (2022).
124. M. J. Novacek, E. E. Cleland, The current biodiversity extinction event: Scenarios for mitigation and recovery. *Proc. Natl. Acad. Sci. U.S.A.* **98**, 5466–5470 (2001).
125. C. H. Basson, O. Levy, M. J. Angilletta, S. Clusella-Trullas, Lizards paid a greater opportunity cost to thermoregulate in a less heterogeneous environment. *Funct. Ecol.* **31**, 856–865 (2017).
126. L. B. Buckley, A. H. Hurlbert, W. Jetz, Broad-scale ecological implications of ectothermy and endothermy in changing environments. *Glob. Ecol. Biogeogr.* **21**, 873–885 (2012).
127. R. E. Buskirk, Zoogeographic patterns and tectonic history of Jamaica and the Northern Caribbean. *J. Biogeogr.* **12**, 445–461 (1985).
128. F. L. Condamine, J. Romieu, G. Guinot, Climate cooling and clade competition likely drove the decline of lamniform sharks. *Proc. Natl. Acad. Sci. U.S.A.* **116**, 20584–20590 (2019).
129. A. Salces-Castellano, J. Patiño, N. Alvarez, C. Andújar, P. Arribas, J. J. Braojos-Ruiz, M. Arco-Aguilar, V. García-Olivares, D. N. Karger, H. López, I. Manolopoulou, P. Oromí, A. J. Pérez-Delgado, W. E. Peterman, K. F. Rijsdijk, B. C. Emerson, Climate drives community-wide divergence within species over a limited spatial scale: Evidence from an oceanic island. *Ecol. Lett.* **23**, 305–315 (2020).
130. N. C. Stenseth, A. Mysterud, G. Ottersen, J. W. Hurrell, K. S. Chan, M. Lima, Ecological effects of climate fluctuations. *Science* **297**, 1292–1296 (2002).
131. J. Clavel, H. Morlon, Accelerated body size evolution during cold climatic periods in the Cenozoic. *Proc. Natl. Acad. Sci. U.S.A.* **114**, 4183–4188 (2017).
132. C. R. Scotese, H. Song, B. J. W. Mills, D. G. van der Meer, Phanerozoic paleotemperatures: The Earth's changing climate during the last 540 million years. *Earth Sci. Rev.* **215**, 103503 (2021).
133. H. Morlon, E. Lewitus, F. L. Condamine, M. Manceau, J. Clavel, J. Drury, RPANDA: An R package for macroevolutionary analyses on phylogenetic trees. *Methods Ecol. Evol.* **7**, 589–597 (2016).
134. A. J. Helmstetter, S. Glemin, J. Käfer, R. Zenil-Ferguson, H. D. S. Sauquet, H. De Boer, L. P. M. J. Dagallier, N. Mazet, E. L. Reboud, T. L. P. Couvreur, F. L. Condamine, Pulled diversification rates, lineages-through-time plots, and modern macroevolutionary modeling. *Syst. Biol.* **71**, 758–773 (2022).
135. C. Simpson, W. Kiessling, "Diversity of life through time" in *Encyclopedia of Life Sciences* (Wiley, 2010).
136. R. G. Fitzjohn, Diversitree: Comparative phylogenetic analyses of diversification in R. *Methods Ecol. Evol.* **3**, 1084–1092 (2012).
137. A. G. Lucaci, J. D. Zehr, D. Enard, J. W. Thornton, S. L. Kosakovsky Pond, Evolutionary shortcuts via multinucleotide substitutions and their impact on natural selection analyses. *Mol. Biol. Evol.* **40**, msad150 (2023).
138. O. Fafioye, O. P. Ayodele, Length-weight relationship and condition factor of four commercial fish species of Oyan Lake, Nigeria. *Exam. Mar. Biol. Oceanogr.* **2**, 10.31031/EIMBO.2018.02.000543 (2018).
139. J. B. Swann, S. J. Holland, M. Petersen, T. W. Pietsch, T. Boehm, The immunogenetics of sexual parasitism. *Science* **369**, 1608–1615 (2020).
140. S. L. Kosakovsky Pond, B. Murrell, M. Fourment, S. D. W. Frost, W. Delport, K. Scheffler, A random effects branch-site model for detecting episodic diversifying selection. *Mol. Biol. Evol.* **28**, 3033–3043 (2011).
141. N. J. Marra, V. P. Richards, A. Early, S. M. Bogdanowicz, P. D. Pavinski Bitar, M. J. Stanhope, M. S. Shivji, Comparative transcriptomics of elasmobranchs and teleosts highlight important processes in adaptive immunity and regional endothermy. *BMC Genomics* **18**, 87 (2017).
142. M. S. Hedrick, S. S. Hillman, What drove the evolution of endothermy? *J. Exp. Biol.* **219**, 300–301 (2016).
143. G. V. Lauder, E. G. Drucker, Forces, fishes, and fluids: Hydrodynamic mechanisms of aquatic locomotion. *News Physiol. Sci.* **17**, 235–240 (2002).

Acknowledgments: We are grateful to R. Norris, B. Frable, Z. Heiple, G. Cuny, D. Saavedra, and E. Miller for input and criticisms during the preparation of our manuscript. We thank D. Rabosky and S. Bauman-Pickering for providing insights regarding the role of modern cetaceans. Computational analyses for this project were performed thanks to the University of Oklahoma Supercomputing Center for Education & Research (OSCER). OSCER Director H. Neeman and OSCER System Administrators J. Speckman, T. Ha, and H. Severini provided valuable technical expertise. **Funding:** This work was supported by the National Science Foundation (NSF) grant (DEB-2144325) awarded to D.A., National Science Foundation (NSF) grant (DEB-2015404) awarded to D.A., National Science Foundation (NSF) grant (DEB-1541491) awarded to R.B.-R., National Science Foundation (NSF) grant (DEB-2225130) awarded to R.B.-R., and National Science Foundation (NSF) grant (DEB-1541552) awarded to G.O. **Author contributions:** Writing—original draft: F.M.-V., D.A., A.G.L., G.O., A.Se., and J.C. Conceptualization: F.M.-V., D.A., A.G.L., and R.B.-R. Investigation: F.M.-V., D.A., D.D., A.G.L., R.B.-R., G.C., and A.Se. Writing—review and editing: F.M.-V., D.A., A.G.L., D.D., C.C.B., L.C.H., A.Sa., E.D.-R., R.B.-R., M.R.-S., M.W.W., G.O., G.C., W.W., M.M., and A.Se. Methodology: F.M.-V., D.A., A.G.L., D.D., R.B.-R., S.L.K.P., A.Se., and J.C. Resources: F.M.-V., D.A., D.D., E.D.-R., C.C.B., R.B.-R., M.W.W., G.O., W.W., and M.M. Funding acquisition: D.A., R.B.-R., M.W.W., and G.O. Data curation: F.M.-V., D.A., A.G.L., C.C.B., E.D.-R., L.C.H., and M.M. Validation: F.M.-V., D.A., A.G.L., R.B.-R., S.L.K.P., G.C., A.Se., and J.C. Supervision: F.M.-V. and D.A. Formal analysis: F.M.-V., D.A., A.G.L., A.Sa., R.B.-R., M.R.-S., S.L.K.P., A.Se., and J.C. Software: F.M.-V., A.G.L., S.L.K.P., A.Se., and J.C., Project administration: F.M.-V. and D.A. Visualization: F.M.-V., D.A., A.Sa., R.B.-R., G.C., S.L.K.P., and A.Se. **Competing interests:** The authors declare that they have no competing interests. **Data and materials availability:** All data needed to evaluate the conclusions in the paper are present in the paper and/or the Supplementary Materials. High-resolution versions of all figures that appear in the main manuscript are available in a Zenodo repository at https://doi.org/10.5281/zenodo.14934749. In addition, all supplementary tables (tables S1 to S27) and datasets (datasets S1 to S11) used in this study are available in a Dryad repository at https://doi.org/10.5061/dryad.ht76hdrpj. Raw sequence reads are available at the National Center for Biotechnology Information Sequence Read Archive BioProject (number PRJNA1262494) at https://ncbi.nlm.nih.gov/bioproject/PRJNA1262494. A repository containing all codes used for phylogenomic assembly and exon capture is available via the Dryad link provided above, as

well as in the following repositories: https://github.com/lilychughes/FishLifeExonHarvesting and https://github.com/lilychughes/FishLifeExonCapture. The codes used for the comparative genomic analyses can be found at https://github.com/veg/Endothermy and https://github.com/veg/Endothermy/tree/main/RER.

Submitted 30 August 2024
Accepted 15 May 2025
Published 25 June 2025
10.1126/sciadv.ads8488